2002-01-01

Characterization of an Acyl-Coa Thioesterase that Functions as a Major Regulator of Peroxisomal Lipid Metabolism

Mary Hunt
Technological University Dublin, mary.hunt@tudublin.ie

Karianne Solaas
Karolinska Institute

Bengt F. Kase
Riskhospitalet, Norway

Stefan E H Alexson
Karolinska Institute

Recommended Citation

Hunt, M., Solaas, K., Frode Kase, B., Alexson, S.: Characterization of an Acyl-CoA Thioesterase That Functions as a Major Regulator of Peroxisomal Lipid Metabolism .J. Biol. Chem. 2002 277: 1128-1138. doi:10.1074/jbc.M106458200

CHARACTERIZATION OF AN ACYL-CoA THIOESTERASE THAT FUNCTIONS AS A MAJOR REGULATOR OF PEROXISOMAL LIPID METABOLISM.

Mary C. Hunt, #Karianne Solaas, *B. Frode Kase and Stefan E. H. Alexson

Department of Medical Laboratory Sciences and Technology, Division of Clinical Chemistry, Karolinska Institutet, Huddinge University Hospital, SE-141 86 Stockholm, Sweden and *Department of Pediatric Research, Rikshospitalet, NO-0027 Oslo, Norway.

Running title: Peroxisomal acyl-CoA thioesterase-2 in lipid metabolism.

Key words: acyl-CoA thioesterase; acyl-CoA; peroxisomes; peroxisome proliferator-activated receptor; HIV-Nef1 binding protein; bile acid-CoA:amino acid *N*-acyltransferase; bile acid-CoA thioesterase; lipid metabolism.

#Present address: Institute for Nutrition Research, University of Oslo, NO-0316 Oslo.

Address for correspondence:
Mary Hunt
Department of Medical Laboratory Sciences and Technology
Division of Clinical Chemistry C1-74
Karolinska Institutet
Huddinge University Hospital
SE-14186 Stockholm
Sweden
Phone: +46-8-58581293
Fax: +46-8-58581260
E-mail: mary.hunt@chemlab.hs.sll.se

Abbreviations: PTE-2, peroxisomal acyl-CoA thioesterase-2; PPARα, peroxisome proliferator-activated receptor alpha; CoASH, coenzyme A; THCA-CoA, trihydroxycoprostanoyl-CoA; CA-CoA, choloyl-CoA; CDCA-CoA, chenodeoxycholoyl-CoA; DMN-CoA, 4,8-dimethyl nonanoyl-CoA; $PGF_{2\alpha}$-CoA, prostaglandin $F_{2\alpha}$-CoA; 2-CH_3-C18-CoA, 2-methylstearoyl-CoA; Mal-CoA, malonyl-CoA; HMG-CoA, 3-hydroxy-3-methyl-glutaryl-CoA; AcAc-CoA, acetoacetyl-CoA; BAAT, bile acid-CoA:amino acid *N*-acyltransferase; ACO, acyl-CoA oxidase; FXR, farnesoid-X-receptor; BSA, bovine serum albumin; PBS, phosphate buffered saline.

ABSTRACT

Peroxisomes function in β-oxidation of very long- and long-chain fatty acids, dicarboxylic fatty acids, bile acid intermediates, prostaglandins, leukotrienes, thromboxanes, pristanic acid and xenobiotic carboxylic acids. These lipids are mainly chain-shortened for excretion as the carboxylic acids or transported to mitochondria for further metabolism. Several of these carboxylic acids are slowly oxidized and may therefore sequester coenzyme A (CoASH). To prevent CoASH sequestration and to facilitate excretion of chain-shortened carboxylic acids, acyl-CoA thioesterases, which catalyze the hydrolysis of acyl-CoAs to the free acid and CoASH, may play important roles. We have here cloned and characterized a peroxisomal acyl-CoA thioesterase from mouse, named PTE-2, which was first isolated as a HIV-1 Nef binding protein in human (Liu et al. J. Biol. Chem. (1997) 272, 13779-13785, Watanabe et al. Biochem. Biophys. Res. Comm. (1997) 238, 234-239). PTE-2 is ubiquitously expressed and induced at mRNA level by treatment with the peroxisome proliferator WY-14,643 and fasting. Induction seen by these treatments was dependent on the peroxisome proliferator-activated receptor alpha (PPARα). Recombinant PTE-2 showed a broad chain-length specificity with acyl-CoAs from short- and medium-, to long-chain acyl-CoAs, and other substrates including trihydroxycoprostanoyl-CoA, hydroxymethylglutaryl-CoA and branched chain acyl-CoAs, all of which are present in peroxisomes. Highest activities were found with the CoA esters of primary bile acids choloyl-CoA and chenodeoxycholoyl-CoA as substrates. PTE-2 activity is inhibited by free CoASH, suggesting that intraperoxisomal free CoASH levels regulate the activity of this enzyme. The acyl-CoA specificity of recombinant PTE-2 closely resembles that of purified mouse liver peroxisomes, suggesting that PTE-2 is the major acyl-CoA thioesterase in peroxisomes. Addition of recombinant PTE-2 to incubations containing isolated mouse liver peroxisomes strongly inhibited bile

acid-CoA: amino acid *N*-acyltransferase activity, suggesting that this thioesterase can interfere with CoASH-dependent pathways. We propose that PTE-2 functions as a key regulator of peroxisomal lipid metabolism.

INTRODUCTION

Peroxisomes are cellular organelles present in all eukaryotic cells. They play an indispensable role in the metabolism of a variety of lipids including very long-chain fatty acids, dicarboxylic fatty acids, bile acids, prostaglandins, leukotrienes, thromboxanes, pristanic acid and xenobiotic fatty acids (for review, see (1,2)). The peroxisomal β-oxidation system contains two sets of enzymes, one of which is involved in the oxidation of branched chain fatty acids and intermediates in the hepatic bile-acid biosynthetic pathway, and consists of one or two branched-chain acyl-CoA oxidase(s), a D-specific bifunctional protein and the sterol carrier-like protein x (SCPx). The second pathway is involved in the oxidation of very long straight-chain fatty acids, CoA esters of prostaglandins, leukotrienes and thromboxanes (prostanoids) and dicarboxylic acids. This system is composed of a straight-chain acyl-CoA oxidase (ACO), an L-specific bifunctional protein and straight-chain 3-ketoacyl-CoA thiolase. However, these two pathways are not mutually exclusive (1). All enzymes in this latter pathway are induced by peroxisome proliferators, whereas the enzymes in the former β-oxidation pathway are not. Peroxisome proliferators are a group of structurally diverse compounds including hypolipidemic drugs, which induce peroxisome proliferation, hepatomegaly and cause hepatocarcinogenesis in rodent liver. These peroxisome proliferators, together with free fatty acids act as ligands for the peroxisome proliferator-activated receptor alpha (PPARα) (3,4). The PPARα is a nuclear receptor that plays a central role in fatty acid metabolism and induces the expression of many enzymes involved in peroxisomal and mitochondrial β-oxidation and ω-oxidation of fatty acids. Targeted disruption of the PPARα gene in mouse has established a key role for this receptor as a mediator of lipid metabolism (5-8) and in the adaptive response to fasting (7-10).

Prior to transport into peroxisomes and β-oxidation, all substrates must be activated to their CoA ester, which occurs at different cellular locations. Long-chain acyl-CoA synthetases are present in different subcellular membranes (11,12) and very long-chain acyl-CoA synthetase in the peroxisomal membrane activates very long- and

long-chain fatty acids and possibly branched-chain fatty acids to their CoA esters. Dicarboxylic fatty acids, prostanoids and di- and trihydroxycoprostanic acid are activated to their CoA esters in the endoplasmic reticulum. These CoA esters are then transported into peroxisomes, possibly via ABC transporters. Peroxisomal β-oxidation of very long- and long-chain fatty acyl-CoAs results in chain-shortening of these esters, and the chain-shortened products can be transported as carnitine esters to mitochondria for further degradation. However, peroxisomes appear to have important roles in β-oxidation of a number of xenobiotic carboxylic acids which may only be partially metabolized in peroxisomes (13,14). The β-oxidation of other CoA esters, such as prostanoids results in chain-shortening in peroxisomes, which are subsequently excreted in urine as the free carboxylic acid (for review see (15)). Similarly the β-oxidation of dicarboxylic acids results in a chain-shortening in peroxisomes with the dicarboxylic acid being excreted in urine as the free acid or as glycine conjugates. Several of these carboxylic acids are only slowly β-oxidized, implying that intraperoxisomal CoASH may be sequestered to such an extent that it becomes limiting. In order to maintain appropriate CoASH levels and to facilitate excretion of chain-shortened carboxylic acids, acyl-CoA thioesterases are likely to play important roles (for review see (16)). The hydrolysis of CoA esters to the free acids requires the presence of an acyl-CoA thioesterase, an enzyme which functions to hydrolyze CoA esters to the free acid and CoASH. To date however, the specific thioesterase(s) active on CoA esters of prostanoids or dicarboxylic acids have not been identified.

Another important reaction that occurs in liver peroxisomes is the formation of bile acids. The primary bile acids, cholic acid and chenodeoxycholic acid, are formed by a number of enzymatic modifications of the cholesterol backbone by P-450 enzymes. The di- or trihydroxycoprostanoyl-CoA (DHCA-CoA or THCA-CoA) formed undergoes a final β-oxidative cleavage of the side-chain in peroxisomes with the release of propionyl-CoA, to form chenodeoxycholoyl-CoA and choloyl-CoA, respectively (17,18). The peroxisomal bile acid-CoA:amino acid *N*-acyltransferase (BAAT) then catalyzes the conjugation of the CoA-activated bile acid to taurine or glycine prior to secretion from liver into bile. Recently, a multiorganellar bile acid-CoA thioesterase activity which hydrolyzes the bile acid-CoA esters to free bile acids and CoASH, has been characterized in human liver peroxisomes (19,20). This bile acid-CoA thioesterase activity described may compete with the BAAT enzyme for

the bile acid-CoA substrate, thereby influencing intracellular levels of free and conjugated bile acids.

The existence of selective acyl-CoA thioesterases or a "broad range" acyl-CoA thioesterase could provide important control points in the oxidation of many peroxisomal substrates, and to regulate intracellular levels of CoA esters and CoASH. This may be especially important during times of high β-oxidation and fatty acid overload, to generate free CoASH necessary for fatty acid β-oxidation to proceed. Acyl-CoA thioesterase activity has indeed been shown to be present in peroxisomes (21-24) and isolated rat brown adipose tissue peroxisomes contain acyl-CoA thioesterase(s) active on short- and medium-chain acyl-CoAs, which are inhibited by CoASH (23). Rat liver peroxisomes showed broad acyl-CoA thioesterase activity on C_2-C_{22} acyl-CoAs and one enzyme was partially purified, which was shown to be most active on myristoyl-CoA (24). To date, several peroxisomal acyl-CoA thioesterases have been cloned from yeast, mouse and human. PTE-Ia and -Ib have been cloned from mouse, which belong to a novel family of Type-I acyl-CoA thioesterases, with related enzymes also in cytosol and mitochondria (25). Acyl-CoA thioesterases have been identified in yeast and human peroxisomes, named PTE1 (26). The human homologue of PTE1 was previously identified as hACTEIII / hTE, a protein that interacted with and activated the HIV-1 Nef protein (27,28). In the present study we have cloned the mouse homologue of PTE1 / hACTEIII / hTE, which we have named mouse peroxisomal acyl-CoA thioesterase 2 (PTE-2). We have characterized this enzyme in detail, in order to examine its putative function in peroxisomal β-oxidation. Characterization of PTE-2 suggests that it is a major thioesterase with an array of functions in peroxisomal lipid metabolism.

EXPERIMENTAL PROCEDURES

Chemicals

[24-^{14}C]-Chenodeoxycholoyl-CoA and [24-^{14}C]-choloyl-CoA (specific activity 48.6 Ci / mol), trihydroxy-cholestanoyl-CoA, 2-methylstearoyl-CoA and prostaglandin $F_{2\alpha}$-CoA were synthesized by the mixed anhydride procedure (29), and the former two CoA esters purified by high-pressure liquid chromatography (HPLC). [24-^{14}C]-Chenodeoxycholic acid and [24-^{14}C]-cholic acid were purchased from DuPont NEN. Optiprep and Maxidens were from Nycomed Pharma AS, Oslo, Norway. Taurine,

chenodeoxycholic acid, cholic acid, all other acyl-CoAs and coenzyme A were from Sigma. Prostaglandin $F_{2\alpha}$ was from Cayman Chemical, Ann Arbor, Michigan.

Animals and treatments

Diurnal variation was investigated in adult male C57 BL/6 mice (B & K, Sollentuna, Sweden). The mice were maintained on a normal chow diet and sacrificed at the time-points indicated. The dark periods were between 18.00 and 06.00 hours. All other treatments were carried out on ten to twelve week old male wild-type or PPARα-null mice on a pure Sv/129 genetic background (derived from the original colony of mixed background mice) (5). These animals were housed in a temperature and light controlled environment. In fasting experiments, mice were maintained on a normal chow diet (R36 Lactamin, Vadstena, Sweden) prior to the start of the experiment and then transferred to new cages and fasted for 24 hours. Alternatively mice were treated with 0.1% WY-14,643 (Calbiochem-Novabiochem International) in the diet for one week. All mice had access to water ad libitum. Animals were sacrificed by CO_2 asphyxiation followed by cervical dislocation, and weighed immediately. Tissues were then excised, weighed and frozen in liquid nitrogen. For subcellular fractionation experiments, livers from untreated wild-type mice were homogenized directly after sacrifice.

Northern blot analysis

Total RNA was isolated from mouse tissue samples using QuickPrep^R Total RNA Extraction Kit (Amersham Pharmacia Biotech Sverige, Uppsala, Sweden) and Northern blot analysis was carried out as described (7). Blots were probed with the full-length cDNA for mouse PTE-2 or a probe for β-actin and were exposed to X-ray film at -70°C.

Identification of human PTE-2 gene

Using human hACTEIII/hTE/hPTE1cDNA sequence (26-28) as search templates, a PAC clone containing approximately 86 kb of human genomic sequence was found to contain the gene encoding PTE-2. This human genomic sequence (Accession No. AL008726) was downloaded from NCBI (http://www.ncbi.nlm.nih.gov). The gene

structure was compiled using Lasergene Software Package and 5' splice donor sites and 3' splice acceptor sites conformed to the general consensus sequences.

cDNA cloning and expression of PTE-2 in *Escherichia coli*

The sequence for hACTEIII / hTE / hPTE1 (26-28) was used to search the mouse EST database and several hits were obtained. The full-length cDNA sequence was compiled from overlapping EST-sequences. The mPTE-2 cDNA was amplified using the following primers: 5'-**CATATG**TCAGCGCCAGAGGGTCTG-3' and 5'-**CATATG**CTATAGCTTACTCTCTGACACCAG-3'. Both primers were constructed with the addition of an *Nde*I site, indicated in bold. The full-length cDNA was amplified by RT-PCR using a template of clofibrate-treated mouse liver total RNA. PCR was performed in a Perkin-Elmer 2600 using the Gene-Amp XL PCR kit (PE Biosystems). Thermal cycling was performed at 98ºC for 10 minutes followed by 35 cycles of 94ºC for 1 min, 64ºC for 1 min and 72ºC for 4 minutes. The resultant PCR product was cloned into the pCR-Script Amp (SK+) vector (Stratagene) and was subsequently sequenced.

The full-length cDNA for PTE-2 was excised from pCR-Script using *Nde*I restriction enzyme and cloned into the *Nde*I site in pET16b vector (Novegen Inc.). Sequence analysis was carried out to confirm the correct orientation. This plasmid was then used to transform BL21(DES3)pLysS cells (Novagen Inc.). For expression of PTE-2, bacteria were cultured in 1 litre Luria-Bertani medium at 37ºC, with addition of ampicillin (50 µg / ml) and chloramphenicol (34 µg / ml) until an A_{600nm} of about 0.6 was reached. Induction of protein expression was performed by addition of 1 mM isopropyl-1-thio-β-D-galactopyranoside and growth was continued overnight at room temperature. The bacteria were centrifuged at 8,000 x g_{max} for 10 min at 4ºC and the pellets were washed with 20 mM Tris, pH 8.0. The pellets were then frozen at -20ºC. Pellets were thawed and resuspended in 20 mM phosphate, 0.5 M sodium chloride and 10 mM imidazole, pH 7.4, and sonicated 5 X 5 seconds, at 5 second intervals. The sonicated bacteria were then centrifuged at 36,000 x g_{max} for 1 hour and the supernatant was used for purification of PTE-2 on a HiTrap™ column (Amersham Pharmacia Biotech Sverige). Following equilibration of the column, the supernatant was applied and the column was washed stepwise with 50 mM, 100 mM, 200 mM and 300 mM imidazole in 20 mM phosphate, 0.5 M sodium chloride, to remove contaminating proteins. The PTE-2 protein was eluted using 500 mM

imidazole, 20 mM phosphate, 0.5 M sodium chloride and was subsequently used for acyl-CoA thioesterase activity measurements. The purity of PTE-2 was examined by SDS-PAGE analysis and Coomassie brilliant blue staining.

Localization of PTE-2 using green fluorescent fusion protein and cell transfection experiments.

Oligonucleotides were designed based on the sequence of the full-length cDNA for mouse PTE-2 for cloning as a fusion protein with green fluorescent protein (GFP), to examine targeting of the protein to peroxisomes. The full-length cDNA was amplified by One Step RNA PCR kit (AMV) (Takara Biomedicals) using the following primers; 5'-ATGTCAGCGCCAGAGGGTC-3' and 5'-CGAGCCAGGCATCTTTCAC-3', and was cloned into the pcDNA3.1/NT-GFP vector (Invitrogen), in-frame with the GFP at the N-terminal end. Sequence analysis was performed using Big Dye Terminator (ABI Prism, PE Biosystems) and was sequenced by Cybergene (Novum, Sweden).

Human skin fibroblasts from a control subject and a Zellweger patient were grown in Eagles Minimum Essential Medium (Sigma), supplemented with 10% Fetal Calf Serum (Life Technologies) and 100 U penicillin/100 µg streptomycin in an atmosphere of 5% CO_2. The Zellweger patient was a first-born, full-term female with muscular hypotonia, convulsions, and dysmorphic characteristics of Zellweger syndrome. The clinical diagnosis was verified by the accumulation of very long-chain fatty acids with a highly elevated C_{26}/C_{22} ratio in cultured fibroblasts. Both control and Zellweger cells were grown overnight in 60 mm dishes on glass coverslips and were transfected with 8 µg mPTE-2/GFP plasmid using Calcium Phosphate method. Transfected cells were grown for 48 hours, washed twice with PBS and fixed in 3.7% paraformaldehyde in PBS for 20 minutes on ice. Cells were permeabilized in 0.5% Triton X-100 in PBS and rewashed in PBS. Following blocking in 2% BSA in PBS, 0.1% Tween-20 for 1 h, cells were incubated with rabbit green fluorescent protein antibody (Molecular Probes, Leiden, The Netherlands) for 1 h and washed 4 times with PBS, 2% BSA and 0.1% Tween-20. Cells were then incubated with CY3 conjugated affinity pure donkey anti-rabbit IgG (Jackson ImmunoResearch) for 1 h. Cells were washed once with PBS, 0.1% Tween-20 (PBS-T) and nuclei were stained with Hoescht 33342 in PBS-T for 10 minutes. Cells were again washed twice in PBS-T and were mounted on glass slides using PPD (100 mg p-

phenylene diamine, 90% glycerol and 10% PBS) and examined in Leica DM IRBE fluroescence microscope, using Hamamatsu C4742-95 camera and C4742-95 Twain Interface software.

Determination of acyl-CoA thioesterase activity

Acyl-CoA thioesterase activity was measured spectrophotometrically at 412 nm with 5,5'-dithiobis(2-nitrobenzoic acid) (DTNB). The medium contained 200 mM potassium chloride, 10 mM Hepes and 0.05 mM DTNB (pH 7.4). An E_{412}=13,600 $m^{-1}cm^{-1}$ was used to calculate the activity. Since PTE-2 thioesterase activity was inhibited at substrate concentrations higher than 5-10 µM with acyl-CoAs longer than C_{10}, bovine serum albumin (BSA) was added to a molar ratio of BSA / acyl-CoA of 4.5:1. The effect of CoASH, DTNB and p-chloromercuribenzoic acid (pCMB) on enzyme activity was measured at 232 nm in phosphate buffered saline. The enzyme kinetics were calculated using Sigma Plot enzyme kinetics programme.

Preparation and characterization of mouse liver subcellular fractions

Livers from wild-type and PPARα-null mice were homogenized as previously described (30) and bile acid-CoA thioesterase activity was measured as in (19). Livers from untreated wild-type mice were fractionated as described (19). The peroxisome-enriched fraction was further fractionated using a 15-45% Optiprep gradient to obtain highly purified peroxisomes. Protein concentrations were determined according to Bradford (31).

Bile acid-CoA:amino acid *N*-acyltransferase assay (BAAT)

The possible interference of PTE-2 on peroxisomal BAAT activity was tested by addition of recombinant PTE-2 to incubations for BAAT activity. The reaction mixture contained the following: 50 mM potassium phosphate buffer (pH 8.0), 25 µM [24-^{14}C]chenodeoxycholoyl-CoA, 20 mM taurine, 60 µg BSA, 2.27 µg mouse liver peroxisomal protein, and 0.6 µg of purified recombinant PTE-2 in a total volume of 150 µl. Control samples were as above, but with inclusion of an equal volume HiTrap™ elution buffer (500 mM imidazole, 0.5 M sodium chloride and 20 mM phosphate, pH 7.4) instead of PTE-2 protein. Following a 10 min preincubation at 37^{o}C, the reaction was started by addition of [24-^{14}C] chenodeoxycholoyl-CoA, and allowed to proceed for 1 hour. The reaction was terminated by addition of 45 µl 1 M

KOH. After 30 min hydrolysis at 70°C, the mixture was acidified using HCl and applied to a Sep-Pak C_{18}-cartridge. The radioactive compounds were eluted with 2-propanol and methanol and analyzed by HPLC using a Beckman ODS 5µ (4.6 mm x 25 cm) column with 20% 30 mM trifluoroacetic acid (adjusted to pH 2.9 with triethylamine) in methanol as mobile phase. The eluents were fractionated and assayed for ^{14}C-radioactivity by liquid scintillation counting.

RESULTS

PTE-2 cloning and sequence analysis

The cDNA isolated for PTE-2 encodes a protein of 320 amino acids, with a calculated molecular mass of 35,886 Da. Alignment of the deduced amino acid sequence for PTE-2 to the homologues in human (26-28), yeast (26), and *E. coli* (32), show the degree of sequence identity between the enzymes (Fig. 1). The mouse and human sequences show 85% sequence identity, the mouse and *E. coli* enzymes show 40% identity at amino acid level, while the yeast and mouse enzymes show 26% sequence identity. The amino acids elucidated to be involved in the active site catalytic triad (33), Asp 233 (D), Ser 255 (S), and Gln 305 (Q) are conserved between species, except for substitution of a threonine for serine in the *E. coli* enzyme. However this substitution should not alter the catalytic site capacity in view of the fact that both amino acids are polar.

Using bioinformatic techniques, we also identified the gene for human PTE-2. The gene was identified on human chromosome 20q12-q13 and comprised 6 exons, spaced by 5 introns, covering approximately 15.5 kb genomic DNA (Fig. 2). The 5' splice donor sites and 3' splice acceptor sites conformed to recognized exon/intron consensus sequences. Sequence analysis of the 5' flanking region of the human PTE-2 identified a putative direct repeat 1 (DR1) element of GGGTCAaAGGTCA, at -438 upstream of the ATG start methionine.

PTE-2 is localized in peroxisomes

The mouse PTE-2 contains a well-characterized consensus peroxisomal Type 1 targeting signal (PTS1) of -SKL (serine, lysine, leucine) at its C-terminal end, which has been shown to target proteins to peroxisomes (34). Previously, human PTE-2 has

been shown to be localized in peroxisomes (26,35) and to test if mouse PTE-2 is peroxisomal, we cloned PTE-2 in-frame with GFP, which leaves the C-terminal -SKL sequence accessible. We transfected this vector into both control fibroblasts and fibroblasts from a Zellweger patient, which are unable to import peroxisomal matrix proteins. Using immunofluorescence microscopy for GFP detection, mPTE-2 showed a punctate pattern of expression in control fibroblasts, indicative of a peroxisomal localization (Fig. 3A). This localization was confirmed with a Tritc-labeled fluorescent secondary antibody to GFP (Fig. 3B). However, in Zellweger fibroblasts, transfection of mPTE-2 resulted in a diffuse GFP expression (Fig. 3D). The transfection of the Zellweger cells was confirmed using a Tritc-labeled fluorescent secondary antibody to GFP, which identified the transfected cells (Fig. 3E). Phase contrast microscopy is also shown in both cases (Fig. 3C & 3F) as a control, indicating other untransfected cells. The strong staining present in the nucleus is Hoescht staining.

Recombinant expression and characterization of PTE-2

The cloning of the cDNA encoding PTE-2 into the *Nde*I site of the pET16B vector results in expression of the PTE-2 as a His-tagged fusion protein, to allow for purification using affinity chromatography. Following purification of PTE-2 on a HiTrap™ column, the purified protein was detected as a single band of approximately 36 kDa in mass on SDS-PAGE gel stained with Coomassie brilliant blue (Fig. 4A). An antibody towards the human PTE1 (a kind gift from Jacob Jones) cross-reacted with the mouse PTE-2, confirming the correct protein (data not shown). The expressed protein was further analyzed by size-exclusion chromatography as described previously (36), using a Superdex HR 200 10/30 column operated in a SMART micropurification system (Amersham Pharmacia Biotech). The recombinant PTE-2 protein eluted as an approximately 70 kDa protein, indicating a dimeric structure of the expressed PTE-2, similar to the crystal structure of the E. coli Thioesterase II enzyme (33).

Following initial enzyme activity characterization of the recombinant protein, it was evident that PTE-2 activity was inhibited at substrate concentrations > 5-10 μM for long-chain acyl-CoAs. However, addition of BSA to an albumin/acyl-CoA ratio of 4.5:1 to the reaction prevented inhibition (Fig. 4B). Recombinant PTE-2 was analyzed for acyl-CoA thioesterase activity, which was determined at several concentrations

with substrates of different chain lengths. Surprisingly, PTE-2 showed similar activity towards all acyl-CoAs tested ranging from C_2 up to C_{20} straight-chain acyl-CoAs, together with activity towards long-chain unsaturated acyl-CoAs (Fig. 4C). Interestingly, PTE-2 also efficiently catalyzed the hydrolysis of CoA esters of bile acids, namely choloyl-CoA and chenodeoxycholoyl-CoA, at an approximately 3-times higher rate than with straight-chain acyl-CoAs, with trihydroxycoprostanoyl-CoA (THCA-CoA) also being hydrolyzed at a high rate. The CoA esters of other substrates found in peroxisomes were also analyzed. PTE-2 hydrolyzed 3-hydroxy-3-methyl-glutaryl-CoA (HMG-CoA), branched-chain CoA esters (4,8-dimethylnonanoyl-CoA and 2-methylstearoyl-CoA), the CoA ester of prostaglandin $F_{2\alpha}$ and acetoacetyl-CoA.

If PTE-2 is a major thioesterase in peroxisomes controlling CoASH levels, it is feasible that it may be directly regulated by CoASH. Indeed PTE-2 activity was strongly inhibited by CoASH with an IC_{50} of approximately 10-15 μM (Fig. 4D). PTE-2 activity was also inhibited by DTNB (IC_{50}≈150 μM) and pCMB (IC_{50}≈ 1 μM), two cysteine-reactive agents (data not shown), however to date a cysteine involved in the active site catalysis has not been identified.

Calculation of the V_{max} and K_m values showed that the K_m for medium- to long-chain acyl-CoAs was in the order of 1.4-6.7 μM, with short chain acyl-CoAs ranging from 8-30 μM (Table I). The K_m for bile acid-CoA esters was in the range of 9-15 μM. PTE-2 also hydrolyzed β-oxidation intermediates such as 2-trans-decenoyl-CoA and 3-hydroxypalmitoyl-CoA, although at approximately 20% of the rates of decanoyl-CoA and palmitoyl-CoA. All K_m values are rather low, strongly suggesting that all these CoA esters are substrates for PTE-2 *in-vivo*.

Recombinant PTE-2 and isolated mouse liver peroxisomes show strikingly similar acyl-CoA thioesterase substrate specificities.

The acyl-CoA thioesterase chain-length specificity was measured in isolated mouse peroxisomes (Fig. 5A). Activity was seen with straight-chain acyl-CoAs from chain length of C_2 up to C_{20}, together with very high activity towards bile-acid CoA esters, THCA-CoA and branched-chain-CoA esters. There was a striking similarity between the acyl-CoA chain-length pattern for the recombinant PTE-2 and the chain length specificity in isolated peroxisomes (Fig. 5B). Superimposing the curves for the

substrate specificities of isolated peroxisomes and that of PTE-2 showed that PTE-2 apparently catalyzes most of the activities seen in peroxisomes, with the only observable difference being the putative presence of an additional acyl-CoA thioesterase in peroxisomes, mainly catalyzing the hydrolysis of C_{12}-C_{14}-CoA. Comparison of the specific activities of recombinant PTE-2 and isolated peroxisomes indicates that PTE-2 constitutes about 1% of total peroxisomal protein.

PTE-2 competes with bile acid-CoA:amino acid *N*-acyltransferase for bile acid-CoA

We examined the ability of recombinant PTE-2 to compete with BAAT for the bile acid-CoA substrate chenodeoxycholoyl-CoA. BAAT activity was measured in highly purified peroxisomes isolated from control mouse liver. Addition of recombinant PTE-2 caused an approximately 80% inhibition of BAAT activity (Table II). This data shows that PTE-2 can compete with BAAT for the bile acid-CoA substrate *in vitro*. We have also tested the ability of recombinant mouse cytosolic acyl-CoA thioesterase I (mCTE-I) (37) to hydrolyze CA-CoA or CDCA-CoA. However, this enzyme showed no detectable activity with CA-CoA or CDCA-CoA, further emphasizing that the bile-acid CoA thioesterase activity of PTE-2 is specific (data not shown).

Choloyl-CoA thioesterase activity is induced in mouse liver in a PPARα-dependent manner

Since PTE-2 very efficiently hydrolyzes CoA esters of bile acids, and PPARα has been shown to be involved in bile acid biosynthesis (38), we investigated the possible regulation of bile acid-CoA thioesterase activity by feeding mice WY-14,643, a potent PPARα activator. In liver homogenates of wild-type mice, choloyl-CoA thioesterase activity was increased 3.5-fold following treatment with WY-14,643 (Fig. 6). However in PPARα-null mouse liver homogenates, this increase in choloyl-CoA thioesterase activity was not evident, showing that the WY-14,643 mediated induction of bile acid-CoA thioesterase activity in mouse liver was PPARα-dependent.

PTE-2 mRNA expression is PPARα-regulated

In view of the fact that PTE-2 can hydrolyze bile-acid CoA esters, together with the fact that choloyl-CoA thioesterase activity was shown to be induced in a PPARα-dependent manner in mouse liver, we used the PPARα-null mouse model to

examine regulation of the PTE-2 at mRNA level. The basal expression of PTE-2 in PPARα-null mice was approximately half that detected in wild-type animals. Treatment of mice with a WY-14,643 containing diet for 1 week resulted in a very strong (> 10 fold) induction of PTE-2 mRNA (Fig. 7A, upper panel). However, this up-regulation was not evident in the PPARα-null mice also treated with WY-14,643, showing that the effect mediated on PTE-2 by peroxisome proliferators is dependent on the PPARα.

The role of the PPARα in the fasting-mediated induction of several genes has also been shown (7-10,38). We examined the effect of fasting on PTE-2 mRNA levels in the PPARα-null mouse model, which resulted in a significant increase in PTE-2 mRNA in liver (Fig. 7A, lower panel). However, this induction was not seen in the PPARα-null mice that were similarly treated.

PTE-2 shows a diurnal regulation of expression

As PTE-2 is regulated by fasting and is therefore under nutritional regulation, we examined if this enzyme could also be under a diurnal regulation. Mice were fed a normal chow diet and were sacrificed every 4th hour commencing at 09.00h. Quantitation of the mRNA signal showed that during the light period (between 06.00h and 18.00h), when animals are less active, the mRNA levels were increased, thus indicating an induction by fasting (Fig. 7B). During the dark period, when feeding mainly takes place (between 18.00h and 06.00h) the mRNA levels declined rapidly, indicating a rapid nutritional regulation in response to refeeding.

PTE-2 mRNA is ubiquitously expressed

The tissue expression of PTE-2 was examined using Northern blot analysis on several different tissues from mouse (Fig. 7C). PTE-2 was ubiquitously expressed as a 1.2 kb transcript in all tissues examined, which is similar to results obtained for expression in human tissues (27). Tissue expression was highest in kidney, liver and testis, with weaker expression evident in heart and muscle. In testis a second transcript was evident at approximately 2 kb, which may be due to splicing events. PTE-2 is therefore widely expressed in tissues, similar to that of the peroxisomal β-oxidation enzymes acyl-CoA oxidase, L-bifunctional enzyme and 3-ketoacyl-CoA thiolase (39).

DISCUSSION

In this study we have cloned and characterized the mouse peroxisomal acyl-CoA thioesterase 2, called PTE-2, which is localized in peroxisomes. This enzyme is the mouse homologue of human PTE1 (26) which was first identified by the yeast two-hybrid system as hACTEIII and hTE, a HIV-1 Nef binding protein (27,28). There is a lot of confusion regarding the nomenclature of acyl-CoA thioesterases, and based on a recent attempt to accomplish a more uniform terminology (16), we propose the name PTE-2 for this acyl-CoA thioesterase, as the nomenclature PTE-I has already been assigned to two enzymes which are members of a novel multi-gene family, with other members in mitochondria and cytosol (25) (Table III). However, the rule applied to the nomenclature of yeast enzymes states that they remain known by the name applied when they were first identified, therefore this enzyme will remain known as PTE1. A PTE2 cloned as a putative peroxisomal enzyme (40) (Table III) shows 100% identity to MTE-I (mitochondrial acyl-CoA thioesterase) without its N-terminal sequence. This MTE-I belongs to a novel family of acyl-CoA thioesterases in human, with localizations also in cytosol and peroxisomes (Hunt et al. Manuscript in preparation).

The HIV-1 Nef which interacts with the thioesterase PTE-2, is a cytosolic 27-kDa myristoylated protein that is required for high viral load and full pathological effect of HIV (41). It is thought that Nef activity triggers endocytosis of CD4 and major histocompatibility complex class-I molecules. Although the interaction of Nef with the acyl-CoA thioesterase is not fully understood, it has been shown that Nef contains sites critical for binding of the human thioesterase, which results in down-regulation of CD4 (35). The binding of Nef to the thioesterase also targets Nef to peroxisomes *in-vivo* and increases thioesterase activity *in-vitro* (27). It was also shown that abolishment of the interaction of the thioesterase with Nef resulted in impairment of Nef biological functions (42). It then became evident that although this thioesterase may have a putative function in the pathogenesis of HIV, the enzyme may also be involved in fatty acid metabolism. In 1999, Jones et al. again characterized this enzyme in human, which they named PTE1, together with a yeast homologue, showing these proteins are targeted to the peroxisomal lumen (26). The yeast PTE1 identified showed regulation at mRNA level by growth on oleate. In

yeast, β-oxidation of fatty acids is confined only to peroxisomes, and growth of yeast on oleate as sole carbon source results in increased expression of peroxisomal enzymes and proliferation of peroxisomes. Disruption of PTE1 in yeast resulted in a loss of approx 80% of total cellular thioesterase activity, demonstrating that PTE1 is the major long-chain acyl-CoA thioesterase in yeast grown on oleate. Furthermore, this deletion impaired growth on oleate, suggesting that efficient β-oxidation in yeast requires the expression of this thioesterase, possibly to closely regulate the intraperoxisomal CoASH levels. Our data now suggest that PTE-2 is in fact a major acyl-CoA thioesterase which can hydrolyze a wide variety of CoA esters in peroxisomes also in the mouse. The difference in acyl-CoA chain-length specificity of PTE-2 in our study compared to previous studies is due to the inclusion of albumin to the thioesterase assay when measuring activity with acyl-CoAs longer than decanoyl-CoA. With addition of albumin, it became evident that PTE-2 hydrolyzes all acyl-CoAs of two carbons up to twenty carbons with very similar V_{max}. The inhibition of PTE-2 activity by CoASH indicates that this enzyme can 'sense' intraperoxisomal CoASH levels and thus when there is a requirement for CoASH, PTE-2 is active, whereas during times of high free CoASH, PTE-2 can be inhibited. Peroxisomes contain a distinct pool of CoASH (43,44), which has been reported to change during fasting and treatment with peroxisome proliferators (45). The extent of CoASH-sequestration may therefore depend on the size of the CoASH-pool, the amount and type of lipids being trapped in the β-oxidation systems in the peroxisome as well as activities of acyl-CoA thioesterases and possibly a recently cloned peroxisomal nudix hydrolase which apparently can hydrolyze CoASH to yield 3',5'-ADP and the corresponding 4'-phosphopantetheine derivative (46).

PTE-2 can have a multitude of functions in regulating peroxisomal lipid metabolism

In the present study we have cloned and characterized the mouse PTE-2 with respect to regulation of expression and kinetic activity. Recombinant PTE-2 hydrolyzed all tested CoA esters, showing an almost complete lack of substrate specificity with respect to the carboxylic acid moiety. The enzyme catalyzes the hydrolysis of straight-chain, saturated and unsaturated acyl-CoAs of two-carbons to 20 carbons in chain-length with roughly similar V_{max}. The enzyme also hydrolyzed other CoA esters such as acetoacetyl-CoA, malonyl-CoA, HMG-CoA, clofibroyl-CoA, THCA-CoA and CoA esters of bile acids, and β-oxidation intermediates. This apparent lack of substrate specificity suggests that the binding site of the enzyme is rather non-specific

with respect to the acyl-moiety and that the enzyme may recognize the CoASH moiety for binding. This is in line with the observed inhibitory effect of free CoASH, the kinetics of which suggested a competitive mode of action, although the data were not fully conclusive. Notably, all the CoA esters tested as substrates for PTE-2 can be expected to be present in peroxisomes as substrates, intermediates or end-products in lipid metabolism. In combination with the strong regulation of expression via PPARα, the PTE-2 thioesterase may have a multitude of functions in peroxisomes as outlined in Fig. 8. Fatty acids and other substrates for β-oxidation in peroxisomes must first be esterified to their CoA ester. CoASH that is appended to poorly oxidizable substrates may cause a trapping of CoASH and thereby prevent the β-oxidation cycle to continue. Thus, PTE-2 may temporarily hydrolyze substrates for the β-oxidation to release CoASH. We also tested CoA esters of β-oxidation intermediates, 2-trans-decenoyl-CoA and 3-hydroxypalmitoyl-CoA. Both these CoA esters were poorer substrates compared to the corresponding straight-chain acyl-CoA: 2-trans-decenoyl-CoA was hydrolyzed at a rate of about 22% of that observed with decanoyl-CoA with the K_m being increased 6-fold and V_{max} being decreased, and 3-hydroxypalmitoyl-CoA which was hydrolyzed at a rate of about 18% of the rate of hydrolysis of palmitoyl-CoA, with the K_m being similar but V_{max} being much lower. The lower activities of PTE-2 with β-oxidation intermediates indicates that the thioesterase preferentially removes the CoA esters of substrates and end-products while β-oxidation intermediates are allowed to be further oxidized.

However, a number of carboxylic acids, such as prostaglandins, leukotrienes and thromboxanes are chain-shortened in peroxisomes and excreted in the urine as the free acids, thus requiring an acyl-CoA thioesterase for these processes. The finding in the present study that PTE-2 readily hydrolyzes the CoA ester of prostaglandin $F_{2\alpha}$ is the first demonstration of an acyl-CoA thioesterase which can have this function.

In the β-oxidation of pristanic acid, the intermediate 4,8-dimethyl-nonanoyl-CoA (DMN) is formed and is transported from the peroxisome to the mitochondria as a carnitine ester, for further oxidation. The high activity of recombinant PTE-2 towards DMN indicates that PTE-2 may also be able to regulate the β-oxidation of branched chain acyl-CoAs in peroxisomes.

PTE-2 is a PPARα-target gene that may regulate bile-acid formation

Bile acids are formed in liver peroxisomes by β-oxidative cleavage of the side-chain of DHCA-CoA or THCA-CoA to chenodeoxycholoyl-CoA and choloyl-CoA, respectively, with the concomitant production of propionyl-CoA. In the last step, bile acid-CoAs are conjugated to taurine or glycine, a reaction catalyzed by the BAAT enzyme that acts as an acyltransferase. In fact the best substrates for PTE-2 were found to be THCA-CoA, CA-CoA and CDCA-CoA. We have now established that PTE-2 is the bile acid-CoA thioesterase previously identified (19,20), suggesting that a major function of the PTE-2 in liver may be in regulation of bile acid formation and excretion. This conclusion is further supported by the competition experiment carried out which showed that addition of a small amount of recombinant PTE-2 to peroxisomes severely suppresses the activity of BAAT, presumably due to consumption of the substrate CDCA-CoA. PPARα has been established as a key regulator of lipid metabolism, but was also shown to be involved in regulation of bile acid metabolism (38), thus connecting the pathways of bile acid and fatty acid metabolism. Upregulation of PTE-2 by WY-14,643, together with the PTE-2 mediated suppression of bile acid conjugation with taurine *in vitro* could imply that PPARα is also involved in regulating bile acid amidation. Indeed, preliminary data shows a reduction in conjugated bile acids in mouse liver following treatment with WY-14,643 (Solaas et al, manuscript in preparation). This functional aspect may be very important in view of the recent interest in the farnesoid-X-receptor (FXR), a nuclear receptor which acts as a biological sensor for the regulation of bile acid biosynthesis, and which is activated by free and conjugated chenodeoxycholic acid (47,48) and cholic acid (49). The FXR/RXR regulates expression of genes involved in bile acid metabolism, such as the human ileal bile acid-binding protein (50) and cholesterol 7α-hydroxylase (51,52). Increased PTE-2 activity would therefore result in an increase in free bile acids, which may subsequently be transported to the nucleus to activate the FXR/RXR heterodimer complex. In this way, PTE-2 may mediate crosstalk between the PPARα and the FXR signalling pathways.

With the identification of the gene for the human PTE-2, a putative peroxisome proliferator-response element (PPRE) was identified at 438 bp upstream of the ATG start site. This site conforms well to the consensus DR1 (AGGTCAnAGGTCA) which has been shown to bind both PPAR/RXR heterodimers and hepatocyte nuclear factor 4α (HNF-4α). It will be of interest to identify if this site is functional in the human promoter in binding these transcription factors, thus leading to possible activation of human PTE-2 by either peroxisome proliferators or fatty acids (the ligands for PPARs

(3,4)), or acyl-CoAs and CoA esters of peroxisome proliferators, (the agonists / antagonists for HNF-4α (53,54)).

Can PTE-2 be considered as an auxilliary β-oxidation enzyme?

In addition to bile-acid intermediates, PTE-2 efficiently hydrolyzes methyl-branched fatty acids (e.g. 4,8-dimethylnonanoyl-CoA and 2-methylstearoyl-CoA) which are substrates of the ”branched-chain” β-oxidation pathway in peroxisomes. Branched-chain CoA esters appear to be excellent substrates for PTE-2, but are generally slowly metabolized via β-oxidation in peroxisomes. At first sight, there appears to be a paradoxical situation that an acyl-CoA thioesterase should facilitate degradation of lipids. However, as outlined before, it is probably very important that appropriate CoASH-levels are maintained in peroxisomes. Such a function is supported by the findings in yeast that deletetion of the gene encoding the yeast homologue PTE1 impairs growth of the PTE1 knock-out strain on oleate. Therefore, a possible function of PTE-2 may be to act as an auxilliary enzyme in β-oxidation of branched-chain fatty acids / bile-acid formation. This β-oxidation pathway is not PPARα-regulated and therefore the PPARα-mediated upregulation of PTE-2 may function in salvaging CoASH for β-oxidation of fatty acids, or alternatively function in (temporarily) decreasing β-oxidation of branched-chain lipids. This could serve to mediate a metabolic cross-talk between PPARα and degradation of this class of lipids in the liver. It should be stressed that it is very likely that PTE-2 can play different functions in different organs which could be related to organ-specific metabolic function of peroxisomes in different tissues.

Is PTE-2 involved in regulation of cholesterol synthesis in peroxisomes?

As outlined above, the PPARα regulation of PTE-2 may confer a metabolic crosstalk between fatty acid degradation and cholesterol metabolism. A similar metabolic crosstalk may occur by PPARα regulation of PTE-2 activity which may interefere with peroxisomal cholesterol biosynthesis. The initial enzymes involved in cholesterol synthesis have been demonstrated to be present in peroxisomes. These enzymes include acetoacetyl-CoA thiolase (55), HMG-CoA synthase (56) and HMG-CoA reductase (57,58). PTE-2 hydrolyzes acetyl-CoA (substrate for acetoacetyl-CoA thiolase), acetoacetyl-CoA (substrate for HMG-CoA synthase) and HMG-CoA (substrate for the HMG-CoA reductase). In addition, while the peroxisomal HMG-

CoA reductase is upregulated two hours into the light cycle (59), PTE-2 is most highly expressed at the end of the light cycle/beginning of the dark cycle, indicating a functionally coordinated regulation of expression i.e. high expression of PTE-2 when HMG-CoA reductase is expressed at low levels.

Role of PTE-2 in regulation of short-chain acyl-CoAs generated from peroxisomal β-oxidation

β-Oxidation of straight-chain and branched-chain fatty acids produces chain-shortened acyl-CoAs which may be transferred to mitochondria (as carnitine esters) for further metabolism, or be excreted in urine. However, for each cycle in the β-oxidation, acetyl-CoA and propionyl-CoA are also produced. Accumulation of propionyl-CoA can be associated with impaired metabolism (60). Propionyl-CoA is formed from the β-oxidation of pristanoyl-CoA and other branched-chain acyl-CoAs, and bile acid intermediates in peroxisomes. This propionyl-CoA may be transferred to carnitine by peroxisomal carnitine octanoyltransferase (COT) for further metabolism in mitochondria, or hydrolyzed to propionic acid. Propionyl-CoA thioesterase activity has previously been identified in peroxisomes (23,24). Our present data show that PTE-2 can efficiently hydrolyze propionyl-CoA with a K_m of <10 μM and a V_{max} of about 3.45 μmol/min/mg protein. Therefore PTE-2 could prevent accumulation of propionyl-CoA and thus release free CoASH for other reactions. In a similar manner, acetyl-CoA units are released during β-oxidation of both very long- and long-chain acyl-CoAs and dicarboxylic acids, and are then hydrolyzed to acetate and excreted to cytosol. Free acetate can account for total acetyl-CoA produced in peroxisomes from dicarboxylic and monocarboxylic acids and acetate production is increased by peroxisome proliferator treatment (61). The production of free acetate from acetyl-CoA requires the hydrolysis by an acyl-CoA thioesterase present in peroxisomes (23,24). Again, recombinant PTE-2 showed high activity towards acetyl-CoA, which constitutes a mechanism to prevent trapping of CoASH in the acetyl-CoA unit.

In summary, we have shown that PTE-2 acts as a general acyl-CoA thioesterase that is responsible for most of the thioesterase activity detected in isolated peroxisomes. Furthermore, PTE-2 is highly regulated by WY-14,643 and fasting which identifies PTE-2 as a novel PPARα-target gene. Based on the regulation of expression and regulation of enzymatic activity by CoASH levels, it is likely that PTE-2 has

important functions in regulating peroxisomal lipid metabolism. We therefore propose that PTE-2 is a major thioesterase found in peroxisomes that may regulate intracellular peroxisomal CoASH levels, controlling β-oxidation of a broad range of acyl-CoA metabolites and the levels of free and conjugated bile acids in liver. PTE-2 could also be a candidate gene for some of the hitherto unidentified disorders of peroxisomal fatty acid metabolism. Targeted disruption of the gene for PTE-2 should provide an interesting model to examine the role of this enzyme in many of the diverse metabolic pathways in peroxisomes.

ACKNOWLEDGEMENTS

This study is supported by the Swedish Society for Medical Research, the Swedish Medical Research Council, the Swedish Natural Science Research Council, Hjärt-Lungfonden and Pharmacia Corporation. We thank Frank Gonzalez and Jeffrey Peters for PPARα-null mice, Jacob Jones for PTE1 antibody, Jan Pedersen for THCA-CoA and 2-methylstearoyl-CoA, Ronald Wanders for 4,8-dimethylnonanoyl-CoA, Kilervo Hiltunen for 2-trans-decenoyl-CoA, Nikolaos Venizelos for 3-hydroxypalmitoyl-CoA, Manfred Held for synthesis of the $PGF_{2\alpha}$-CoA ester, and Kjell Hultenby for GFP antibody. We also gratefully acknowledge the advice and assistance of Cecilia Rustum and Einar Hallberg regarding GFP experiments and for the GFP secondary antibody.

REFERENCES

1. Van Veldhoven, P. P., and Mannaerts, G. P. (1999) *Adv. Exp. Med. Biol.* **466,** 261-272
2. Reddy, J. K., and Hashimoto, T. (2001) *Annu. Rev. Nutr.* **21,** 193-230
3. Forman, B. M., Chen, J., and Evans, R. M. (1997) *Proc. Natl. Acad. Sci. U.S.A.* **94,** 4312-4317
4. Kliewer, S. A., Sundseth, S. S., Jones, S. A., Brown, P. J., Wisely, G. B., Koble, C. S., Devchand, P., Wahli, W., Willson, T. M., Lenhard, J. M., and Lehmann, J. M. (1997) *Proc. Natl. Acad. Sci. U.S.A.* **94,** 4318-4323
5. Lee, S. S., Pineau, T., Drago, J., Lee, E. J., Owens, J. W., Kroetz, D. L., Fernandez-Salguero, P. M., Westphal, H., and Gonzalez, F. J. (1995) *Mol. Cell. Biol.* **15,** 3012-3022
6. Aoyama, T., Peters, J. M., Iritani, N., Nakajima, T., Furihata, K., Hashimoto, T., and Gonzalez, F. J. (1998) *J. Biol. Chem.* **273,** 5678-5684
7. Hunt, M. C., Lindquist, P. J. G., Peters, J. M., Gonzalez, F. J., Diczfalusy, U., and Alexson, S. E. H. (2000) *J. Lipid Res.* **41,** 814-823

8. Kroetz, D. L., Yook, P., Costet, P., Bianchi, P., and Pineau, Y. (1998) *J. Biol. Chem.* **273,** 31581-31589
9. Kersten, S., Seydoux, J., Peters, J. M., Gonzalez, F. J., Desvergne, B., Wahli, W. (1999) *J. Clin. Invest.* **103,** 1489-1498
10. Leone, T. C., Weinheimer, C. J., Kelly, D. P. (1999) *Proc. Natl. Acad. Sci. U.S.A.* **96,** 7473-7478
11. Lewin, T. M., Kim, J. H., Granger, D. A., Vance, J. E., and Coleman, R. A. (2001) *J. Biol. Chem.* **276,** 24674-24679
12. Gargiulo, C. E., Stuhlsatz-Krouper, S. M., and Schaffer, J. E. (1999) *J. Lipid. Res.* **40,** 881-892
13. Yamada, J., Itoh, S., Horie, S., Watanabe, T., and Suga, T. (1986) *Biochem. Pharmacol.* **35,** 4363-4368
14. Yamada, J., Ogawa, S., Horie, S., Watanabe, T., and Suga, T. (1987) *Biochim. Biophys. Acta* **921,** 292-301
15. Diczfalusy, U. (1994) *Prog. Lipid Res.* **33,** 403-428
16. Hunt, M. C., and Alexson, S. E. H. (2001) *Prog. Lipid Res.* **In press.,**
17. Pedersen, J. I., and Gustafsson, J. (1980) *FEBS Lett.* **121,** 345-348
18. Kase, F., Björkhem, I., and Pedersen, J. I. (1983) *J. Lipid Res.* **24,** 1560-1567
19. Solaas, K., Ulvestad, A., Söreide, O., and Kase, B. F. (2000) *J. Lipid Res.* **41,** 1154-1162
20. Solaas, K., Sletta, R. J., Søreide, O., and Kase, B. F. (2000) *Scand. J. Clin. Invest.* **60,** 91-102
21. Osmundsen, H., Neat, C. E., and Borrebaek, B. (1980) *Int. J. Biochem.* **12,** 625-30
22. Berge, R. K., Flatmark, T., and Osmundsen, H. (1984) *Eur. J. Biochem.* **141,** 637-644
23. Alexson, S. E. H., Osmundsen, H., and Berge, R. K. (1989) *Biochem. J.* **262,** 41-46
24. Wilcke, M., and Alexson, S. E. H. (1994) *Eur. J. Biochem.* **222,** 803-811
25. Hunt, M. C., Nousiainen, S. E. B., Huttunen, M. K., Orii, K., Svensson, L. T., and Alexson, S. E. H. (1999) *J. Biol. Chem.* **274,** 34317-34326
26. Jones, J. M., Nau, K., Geraghty, M. T., Erdmann, R., and Gould, S. J. (1999) *J. Biol. Chem.* **274,** 9216-9223
27. Watanabe, H., Shiratori, T., Shoji, H., Miyatake, S., Okazaki, Y., Ikuta, K., Sato, T., and Saito, T. (1997) *Biochem. Biophys. Res. Comm.* **238,** 234-239
28. Liu, L. X., Margottin, F., Le Gall, S., Schwartz, O., Selig, L., Benarous, R., and Benichou, S. (1997) *J. Biol. Chem.* **272,** 13779-13785
29. Shah, P. P., and Staple, E. (1968) *Steroids* **12,** 571-575
30. Prydz, K., Kase, B. F., Björkhem, I., and Pedersen, J. I. (1986) *J. Lipid Res.* **27,** 622-628
31. Bradford, M. M. (1976) *Anal. Biochem.* **72,** 248-254
32. Naggert, J., Narasimhan, M. L., DeVeaux, L., Cho, H., Randhawa, Z. I., Cronan, J. E., Green, B. N., and Smith, S. (1991) *J. Biol. Chem.* **266,** 11044-11050
33. Li, J., Derewenda, U., Dauter, Z., Smith, S., and Derewenda, Z. S. (2000) *Nature Struct. Biol.* **7,** 555-559
34. Gould, S. J., Keller, G. A., Hosken, N., Wilkinson, J., and Subramani, S. (1989) *J. Cell Biol* **108,** 1657-64

35. Cohen, G. B., Rangan, V. S., Chen, B. K., Smith, S., and Baltimore, D. (2000) *J. Biol. Chem.* **275,** 23097-23105
36. Svensson, L. T., Wilcke, M., and Alexson, S. E. H. (1995) *Eur. J. Biochem.* **230,** 813-820
37. Lindquist, P. J. G., Svensson, L. T., and Alexson, S. E. H. (1998) *Eur. J. Biochem.* **251,** 631-640
38. Hunt, M. C., Yang, Y. Z., Eggertsen, G., Carneheim, C. M., Gåfvels, M., Einarsson, C., and Alexson, S. E. H. (2000) *J. Biol. Chem.* **37,** 28947-28953
39. Nemali, M. R., Usuda, N., Reddy, M. K., Oyasu, K., Hashimoto, T., Osumi, T., Rao, M. S., and Reddy, J. K. (1988) *Cancer Res.* **48,** 5316-5324
40. Jones, J. B., and Gould, S. J. (2000) *Biochem. Biophys. Res. Comm.* **275,** 233-240
41. Kestler, W. H., Ringler, D. J., Mori, K., Panicali, D. L., Shegal, P. K., Daniel, M. D., and Desrosiers, R. C. (1991) *Cell* **65,** 651-662
42. Liu, L. X., Heveker, N., Fackler, O. T., Arold, S., Le Gall, S., Janvier, K. P., B. M., Dumas, C., Schwartz, O., Benichou, S., and Benarous, R. (2000) *J. Virology* **74,** 5310-5319
43. Van Broekhoven, A., Peeters, M. C., Debeer, L. J., and Mannaerts, G. P. (1981) *Biochem. Biophys. Res. Commun.* **100,** 305-312
44. Van Veldhoven, P. P., and Mannaerts, G. P. (1986) *Biochem. Biophys. Res. Commun.* **139,** 1195-1201
45. Horie, S., Isobe, M., and Suga, T. (1986) *J. Biochem.* **99,** 1345-1352
46. Gasmi, L., and McLennan, A. G. (2001) *Biochem. J.* **357,** 33-38
47. Makishima, M., Okamoto, A. Y., Repa, J. J., Tu, H., Learned, R. M., Luk, A., Hull, M. V., Lustig, K. D., Mangelsdorf, D. J., and Shan, B. (1999) *Science* **284,** 362-365
48. Parks, D. J., Blanchard, S. G., Bledsoe, R. K., Chandra, G., Consler, T. G., Kliewer, S. A., Stimmel, J. B., Willson, T. M., Zavacki, A. M., Moore, D. D., and Lehmann, J. M. (1999) *Science* **284,** 1285-1286
49. Wang, H., Chen, J., Holoister, K., Sowers, L. C., and Forman, B. M. (1999) *Mol. Cell* **5,** 543-553
50. Grober, J., Zaghini, I., Fujii, H., Jones, S. A., Kliewer, S. A., Willson, T. M., Ono, T., and Besnard, P. (1999) *J. Biol. Chem.* **274,** 29749-29754
51. del Castillo-Olivares, A., and Gil, G. (2000) *Nucleic Acids Res.* **28,** 3587-3593
52. Chiang, J. Y., Kimmel, R., Weinberger, C., and Stroup, D. (2000) *J. Biol. Chem.* **275,** 10918-10924
53. Hertz, R., Magenheim, J., Berman, I., and Bar-Tana, J. (1998) *Nature* **392,** 512-516
54. Hertz, R., Sheena, V., Kalderon, B., Berman, I., and Bar-Tana, J. (2001) *Biochem. Pharmacol.* **61,** 1057-1062
55. Thompson, S. L., and Krisans, S. K. (1990) *J. Biol. Chem.* **265,** 5731-5735
56. Olivier, L. M., Kovacs, W., Masuda, K., Keller, G. A., and Krisans, S. K. (2000) *J. Lipid Res.* **41,** 1921-1935
57. Keller, G. A., Barton, M. C., Shapiro, D. J., and Singer, S. J. (1985) *Proc. Natl. Acad. Sci. U.S.A* **82,** 770-774

58. Keller, G. A., Pazirandeh, M., and Krisans, S. (1986) *J. Cell. Biol.* **103,** 875-886
59. Rusnak, N., and Krisans, S. K. (1987) *Biochem. Biophys. Res. Commun.* **148,** 890-895
60. Brass, E. P. (1994) *Chem. Biol. Interact.* **90,** 203-214
61. Leighton, F., Bergseth, S., Rørtveit, T., Christiansen, E. N., and Bremer, J. (1989) *J. Biol. Chem.* **264,** 10347-10350

FIGURE LEGENDS

Fig. 1 Sequence alignment of acyl-CoA thioesterases from mouse, human, yeast and *E. coli.* Alignment of mouse PTE-2, human PTE1 (26-28), yeast (S.c) PTE1 (26) and E. coli Thioesterase II (32) amino acid sequences was performed using the Clustal X method. Amino acids conserved between the thioesterase sequences are boxed in black. The active site aspartic acid (D) 233, serine / threonine (S / T) 255 and glutamine (Q) 305 residues of the catalytic triad are all indicated with closed triangles.

Fig. 2 Gene organization for human PTE-2. The gene organization for human PTE-2 was determined as outlined in EXPERIMENTAL PROCEDURES. Individual exon sizes are shown (boxes) while intron sizes are shown underneath. A putative DR1 element is indicated at -438 upstream of the ATG start site.

Fig. 3: PTE-2 is a peroxisomal matrix protein. Human skin fibroblasts transfected with mPTE-2 / GFP were processed for immunofluorescence microscopy by fixing and permeabilizing with 0.5% Triton X-100. The distribution of mPTE-2 was examined in control fibroblasts using GFP fluorescence (A) and Tritc-labeled anti-GFP antibody (B). The distribution of mPTE-2 in Zellweger fibroblasts was also carried out using GFP fluorescence (D) and Tritc-labeled anti-GFP antibody (E). Phase contrast microscopy is shown in (C) and (F).

Fig. 4 Kinetic characterization of recombinant mouse PTE-2. Expression of recombinant PTE-2 in pET16b vector was induced as described in EXPERIMENTAL PROCEDURES. **(A)** Recombinant PTE-2 was purified on a HiTrap™ column and the purified protein was subjected to SDS-PAGE analysis and staining with Coomassie brilliant blue. Sizes of molecular weight markers are indicated. **(B)** Enzyme activity measurements were determined using purified PTE-2 as an enzyme source. Acyl-CoA thioesterase activity was measured with various concentrations of palmitoyl-CoA ± BSA at an albumin to substrate molar ratio of 4.5:1. **(C)** Acyl-CoA thioesterase activity on various CoA esters using purified PTE-2 as an enzyme source. Acyl-CoA thioesterase activity was measured with 10 μM of the indicated CoA ester, in the presence of BSA at a substrate to albumin molar ratio of 1:4.5 for CoA esters longer than C_{10}. Cn, number of carbons; THCA-CoA, trihydroxycoprostanoyl-CoA; CA-CoA, choloyl-CoA; CDCA-CoA, chenodeoxycholoyl-CoA; DMN, 4,8-dimethyl nonanoyl-CoA; $PGF_{2\alpha}$, prostaglandin $F_{2\alpha}$; 2-CH_3-C18, 2-methylstearoyl-CoA; Mal, malonyl-CoA;

HMG, 3-hydroxy-3-methyl-glutaryl-CoA; AcAc, acetoacetyl-CoA. **(D)** Inhibition of PTE-2 activity by CoASH. Acyl-CoA thioesterase activity was measured at 232 nm as described in EXPERIMENTAL PROCEDURES. The activity was measured using octanoyl-CoA as substrate, to avoid the required addition of BSA, which will strongly interfere at 232 nm when measuring activity with longer acyl-CoAs. CoASH was added to the enzyme assay at concentrations indicated.

Fig. 5 Acyl-CoA thioesterase substrate specificity in purified peroxisomes and for recombinant PTE-2. (A) Acyl-CoA thioesterase activity measurements were determined in 2.27 µg purified peroxisomes from wild-type mice treated with 0.1% WY-14,643 for one week, using 25 µM of various acyl-CoA esters. **(B)** Enzyme activity measurements were determined using purified PTE-2 as an enzyme source, using 0.3-1.2 µg of recombinant PTE-2 and 25 µM acyl-CoA as substrate. THCA, trihydroxycoprostanoyl-CoA; CA, choloyl-CoA; CDCA, chenodeoxycholoyl-CoA; DMN, 4,8-dimethyl nonanoyl-CoA.

Fig. 6 Bile acid-CoA thioesterase activity is increased in mouse liver homogenates by WY-14,643 treatment. Specific choloyl-CoA thioesterase activity was measured as described in EXPERIMENTAL PROCEDURES in homogenates from untreated PPARα wild-type (+/+) and null (-/-) mice and mice treated with 0.1% WY-14,643 (WY) for one week.

Fig. 7 Northern blot analysis of PTE-2 mRNA expression in mouse liver. (A) Upper panel. Groups of six PPARα-null mice (-/-) or age matched wild-type mice (+/+) were fed 0.1% WY-14,643 for one week, while control animals had access to normal chow diet ad libitum. Mice were sacrificed and total RNA was isolated from liver. Northern blot analysis was carried out on 20 µg total RNA using α-^{32}P-labeled cDNA probe for PTE-2 as described in EXPERIMENTAL PROCEDURES. A representative blot with two samples per group is shown together with the ethidium bromide staining of the blot with positions of the 28S and 18S bands indicated. **Lower Panel**: Northern blot analysis of mouse liver total RNA from control mice or mice fasted for 24 hours. **(B)** PTE-2 mRNA expression shows diurnal variation. C57 BL/6 mice were maintained on a normal chow diet ad libitum and were sacrificed at the time-points indicated. The light period was between 06.00 and 18.00 and the dark period between 18.00 and 06.00. Northern blot analysis was carried out on 20 µg total RNA using α-^{32}P-labeled probes for PTE-2 and β-actin. Filters were exposed to X-ray

film and signals were quantified using Image Master Software 3.0. The mean of PTE-2/actin mRNA ± range for two animals is shown. **(C)** Tissue expression of PTE-2 mRNA. Total RNA was isolated from various tissues of Sv129 male mice. Northern blot analysis was carried out on 20 µg total RNA using α-^{32}P-labeled cDNA probe for PTE-2 as described in EXPERIMENTAL PROCEDURES. Ethidium bromide (Et Br) staining of the gel shows even loading of samples.

Fig. 8 Model for putative functions of PTE-2 in peroxisomes. PTE-2 may function as an auxillary enzyme in β-oxidation of a number of substrates in peroxisomes. Abbreviations used: VLCFA, very long-chain fatty acids: THCA-CoA, trihydroxycoprostanoyl-CoA; BAAT, bile acid-CoA:amino acid *N*-acyltransferase; PTE-2, peroxisomal acyl-CoA thioesterase 2; COT, carnitine octanoyl-transferase; PG, prostaglandins: LT, leukotrienes; Tb, thromboxanes; FFA, free fatty acid; Cn, carnitine; DMN-CoA, 4,8-dimethyl nonanoyl-CoA.

Table I: Calculated K_m and V_{max} values for recombinant PTE-2.
Thioesterase activity with different CoA esters were measured at different substrate concentrations. Activities were measured as described under 'EXPERIMENTAL PROCEDURES' using 0.3-1.2 µg purified recombinant PTE-2. K_m and V_{max} values were calculated using Sigma Plot Enzyme Kinetic programme.The activity of PTE-2 with two β-oxidation intermediates, 2-trans-decenoyl-CoA and 3-hydroxy-palmitoyl-CoA, were compared to the activities with decanoyl-CoA and palmitoyl-CoA, respectively, all measured at 25 µM.

CoA ester	**K_m**	**V_{max}**
Straight chain acyl-CoA	**µM**	**µmol/min/mg**
Acetyl	29.4	4.6
Propionyl	8.0	3.45
Butyryl	22.6	2.6
Hexanoyl	23.4	5.6
Octanoyl	6.9	3.9
Decanoyl	2.9	3.8
Lauroyl	2.8	3.0
Myristoyl	2.5	3.6
Myristoleoyl	3.5	3.2
Palmitoyl	1.7	3.4
Palmitoleoyl	1.4	2.7
Stearoyl	2.7	3.2
Oleoyl	1.6	3.1
Linoleoyl	2.3	2.3
Arachidoyl	4.2	2.2
Arachidonoyl	6.7	1.6
"Bile acids"		
Trihydroxycoprostanoyl	6.3	8.1
Choloyl	14.6	17.9
Chenodeoxycholoyl	8.8	17.1
Others		
4,8-dimethyl nonanoyl	5.5	10.69
Prostaglandin $F_{2\alpha}$	0.92	2.25
2-methyl stearoyl	1.9	1.65
Malonyl	12.9	1.19
3-hydroxy-3-methyl-glutaryl	22.9	2.85
Acetoacetyl	22.9	6.0
Clofibroyl-CoA	n.d.	1.65
β-oxidation Intermediates		
2-trans-decenoyl	17.3	2.55
3-hydroxypalmitoyl	2.7	0.77

Table II: Specific activity of bile acid-CoA:amino acid *N*-acyltransferase (BAAT) in purified peroxisomes from untreated wild-type mice. Addition of recombinant PTE-2 to the incubation mixture and detection of tauro-chenodeoxycholic acid formation was as described in 'EXPERIMENTAL PROCEDURES'. All samples were measured in duplicate.

	BAAT activity (nmol/mg/min)	**BAAT activity (%)**
Control	6.10	100
+ PTE-2 (0.6 µg)	1.06	17

Table III: Nomenclature for peroxisomal acyl-CoA thioesterases

Enzyme (Proposed Name)	Species	Localization	Other Name	Cloned	Reference
mPTE-Ia	mouse	peroxisomal	--	gene	(25)
mPTE-Ib	mouse	peroxisomal	--	gene	(25)
hPTE-I	human	peroxisomal	--	gene	Hunt et al. Manuscript in preparation.
MTE-I	human	putative mitochondrial	PTE2	cDNA	(40)
PTE1	yeast	peroxisomal	--	cDNA	(26)
PTE-2	human	peroxisomal	hTE	cDNA	(28)
		peroxisomal	hACTEIII	cDNA	(27)
		peroxisomal	PTE1	cDNA	(26)
		peroxisomal		gene	this article
	mouse	peroxisomal		cDNA	this article

Hunt et al
Fig. 1

Hunt et al
Fig. 2

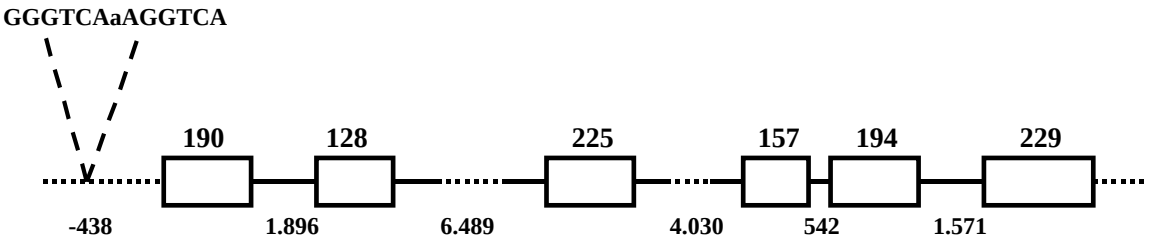

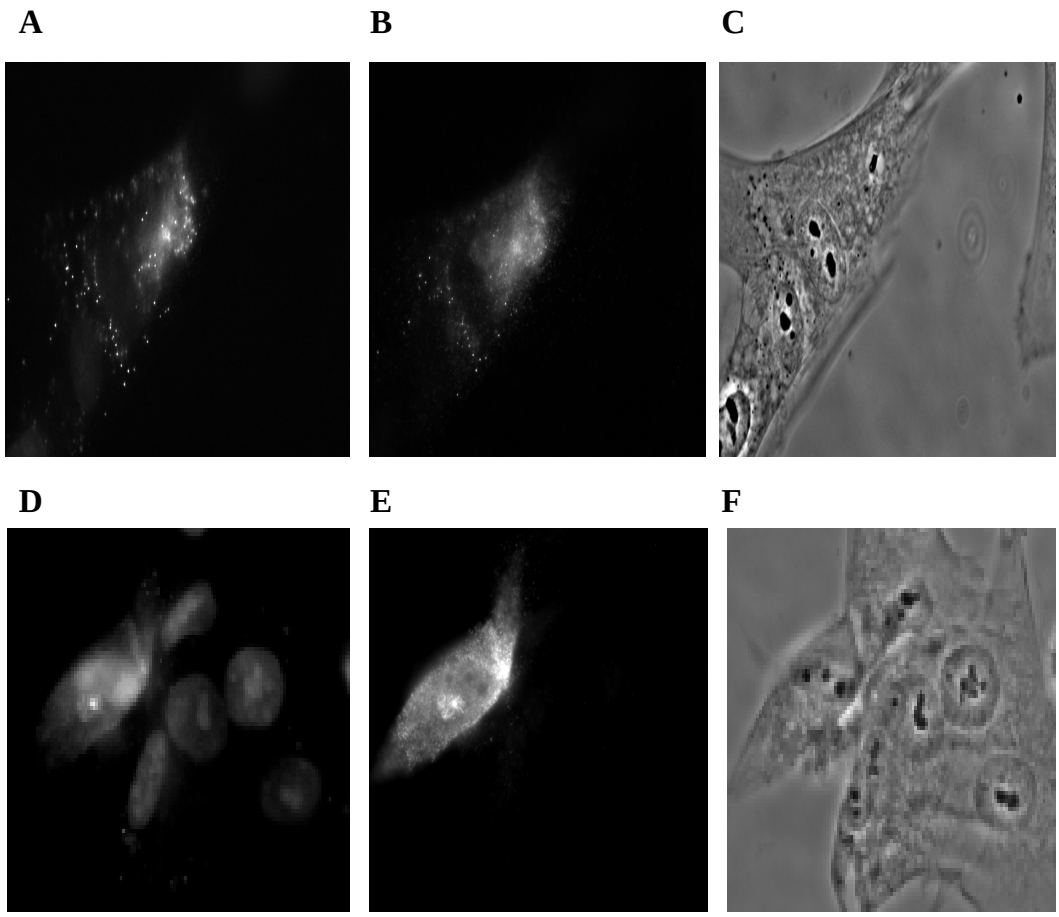
A
B
C
D
E
F

Hunt et al
Fig. 4A

A

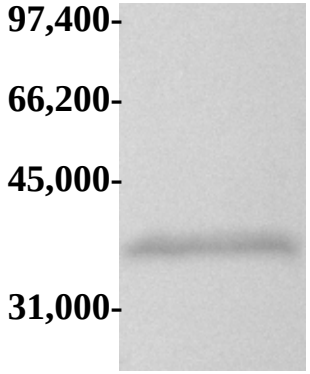

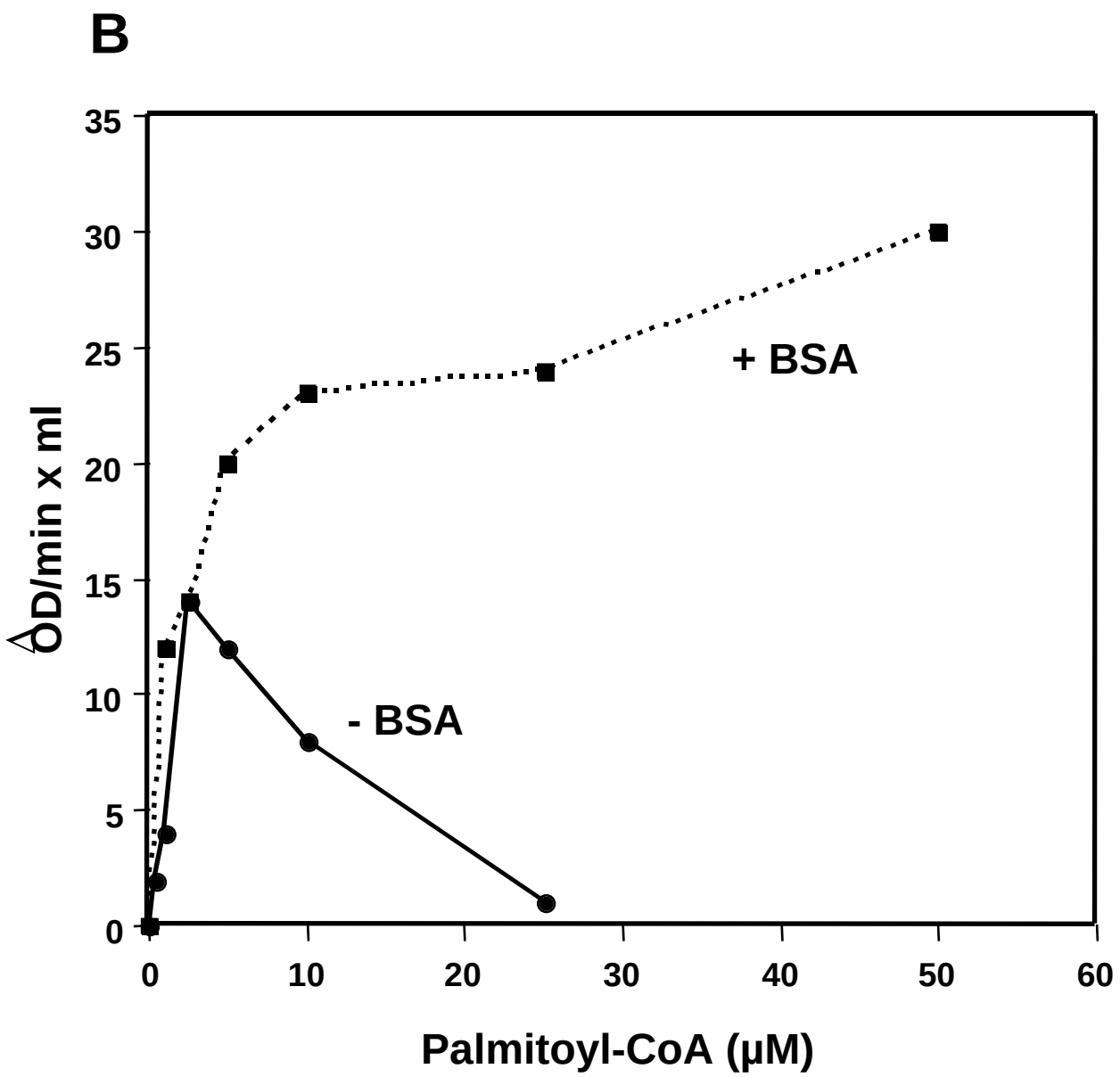
B
35
30
25
20
15
10
5
0
ΔOD/min x ml
+ BSA
- BSA
0
10
20
30
40
50
60
Palmitoyl-CoA (μM)

C

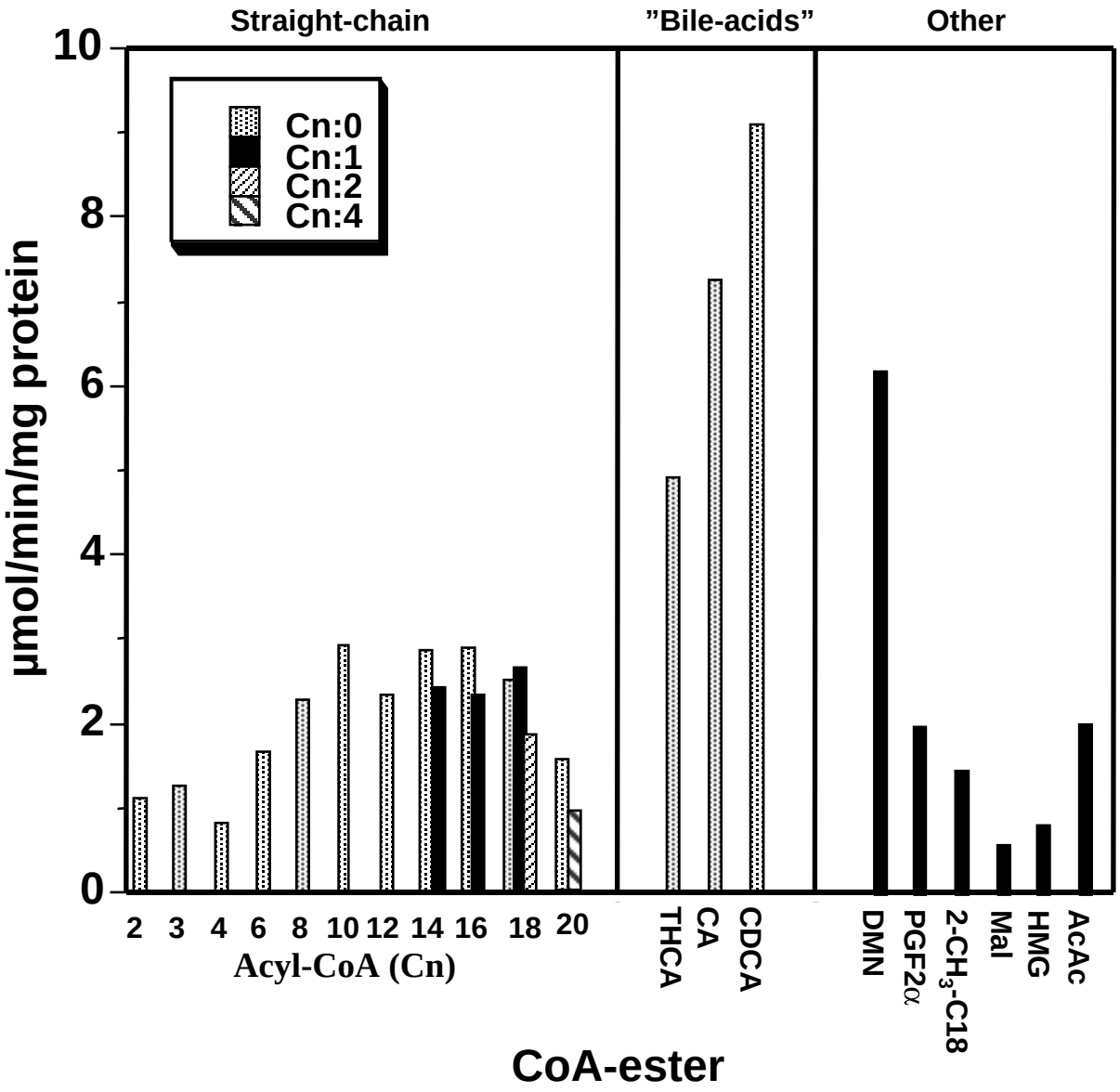
Straight-chain
"Bile-acids"
Other
Cn:0
Cn:1
Cn:2
Cn:4
µmol/min/mg protein
0
2
4
6
8
10
2 3 4 6 8 10 12 14 16 18 20
Acyl-CoA (Cn)
THCA
CA
CDCA
DMN
PGF2α
2-CH3-C18
Mal
HMG
AcAc
CoA-ester

Hunt et al
Fig. 4D

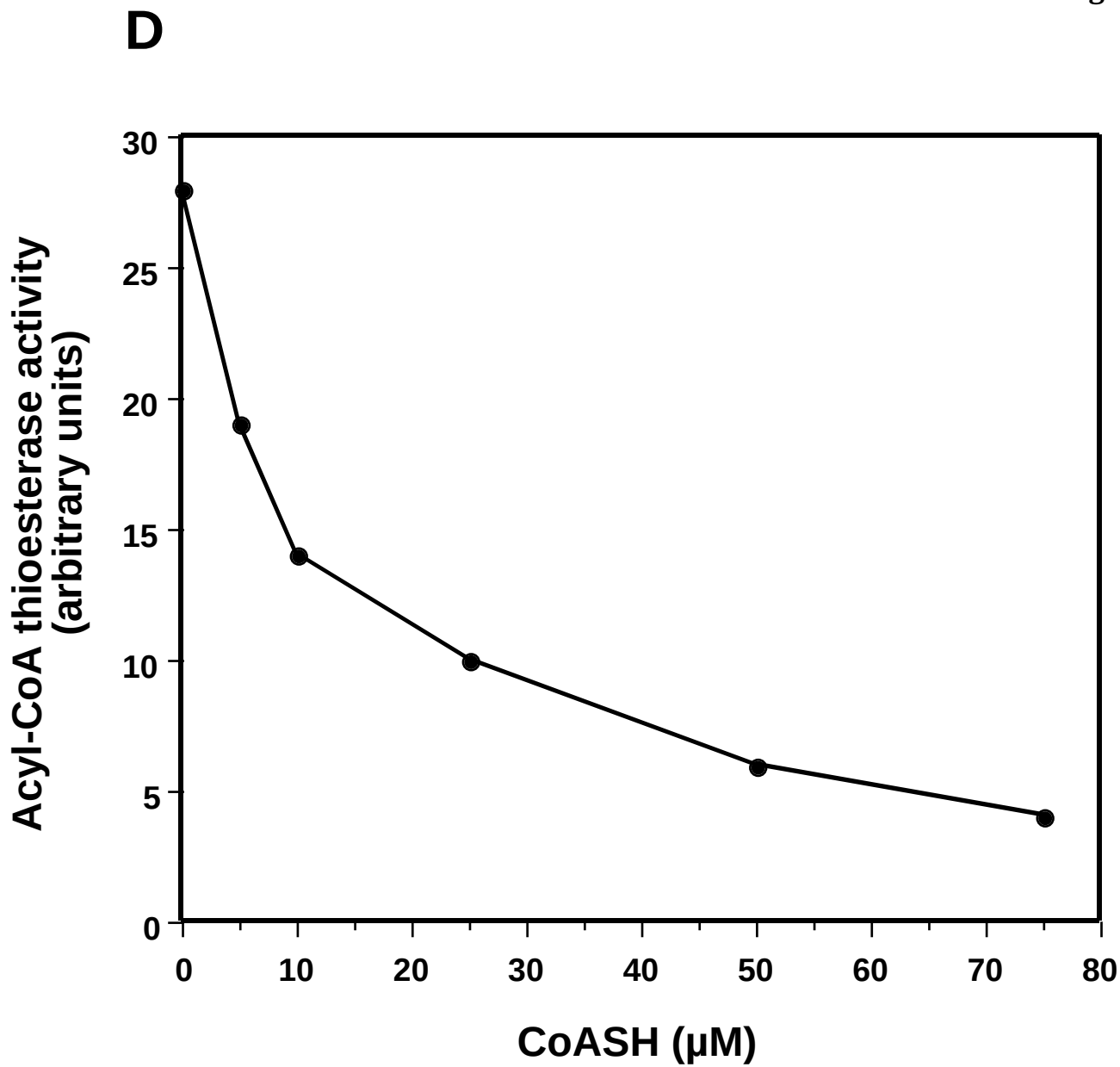

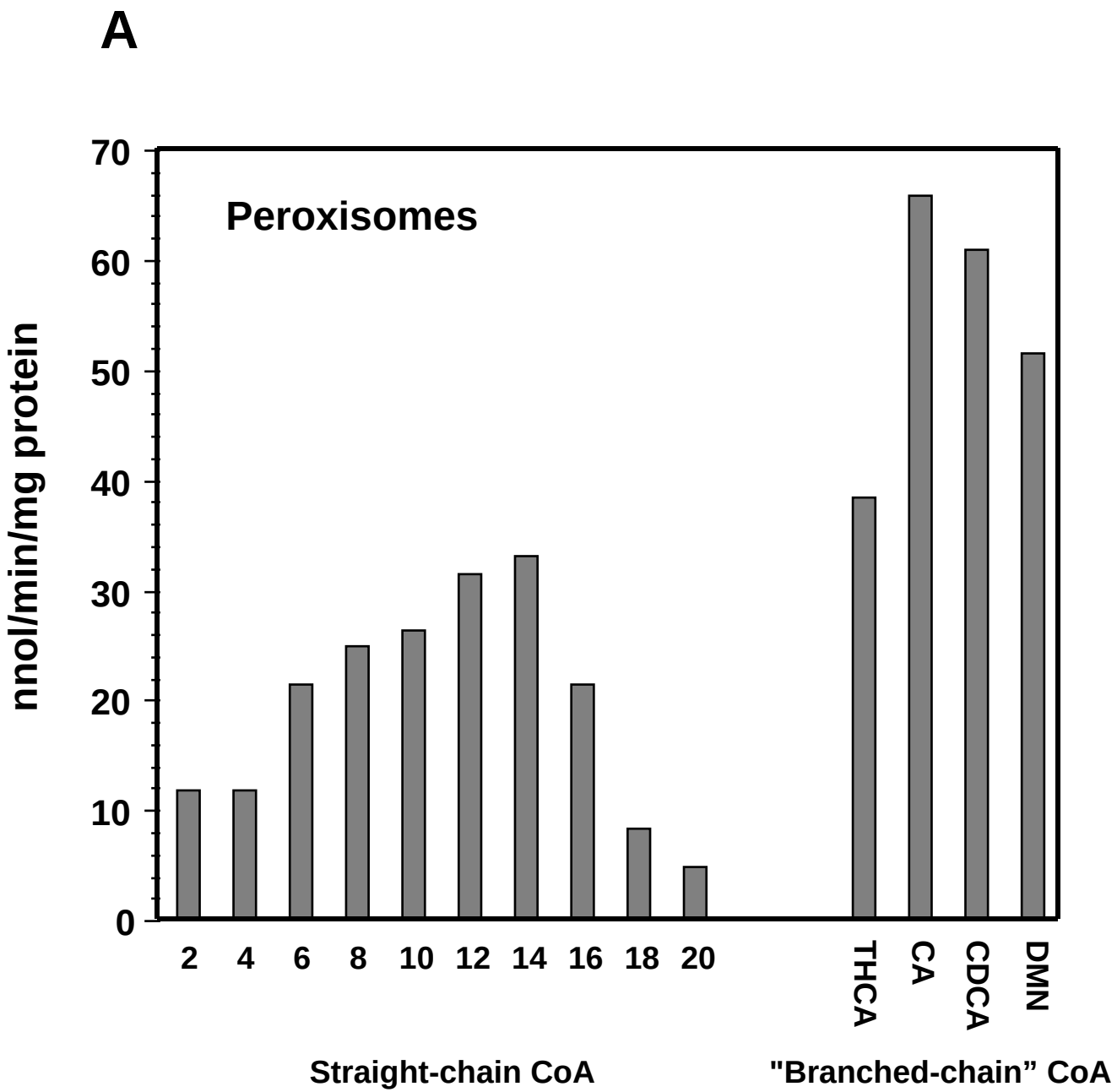
A
Peroxisomes
nnol/min/mg protein
70
60
50
40
30
20
10
0
2
4
6
8
10
12
14
16
18
20
THCA
CA
CDCA
DMN
Straight-chain CoA
"Branched-chain" CoA

Hunt et al
Fig. 5B

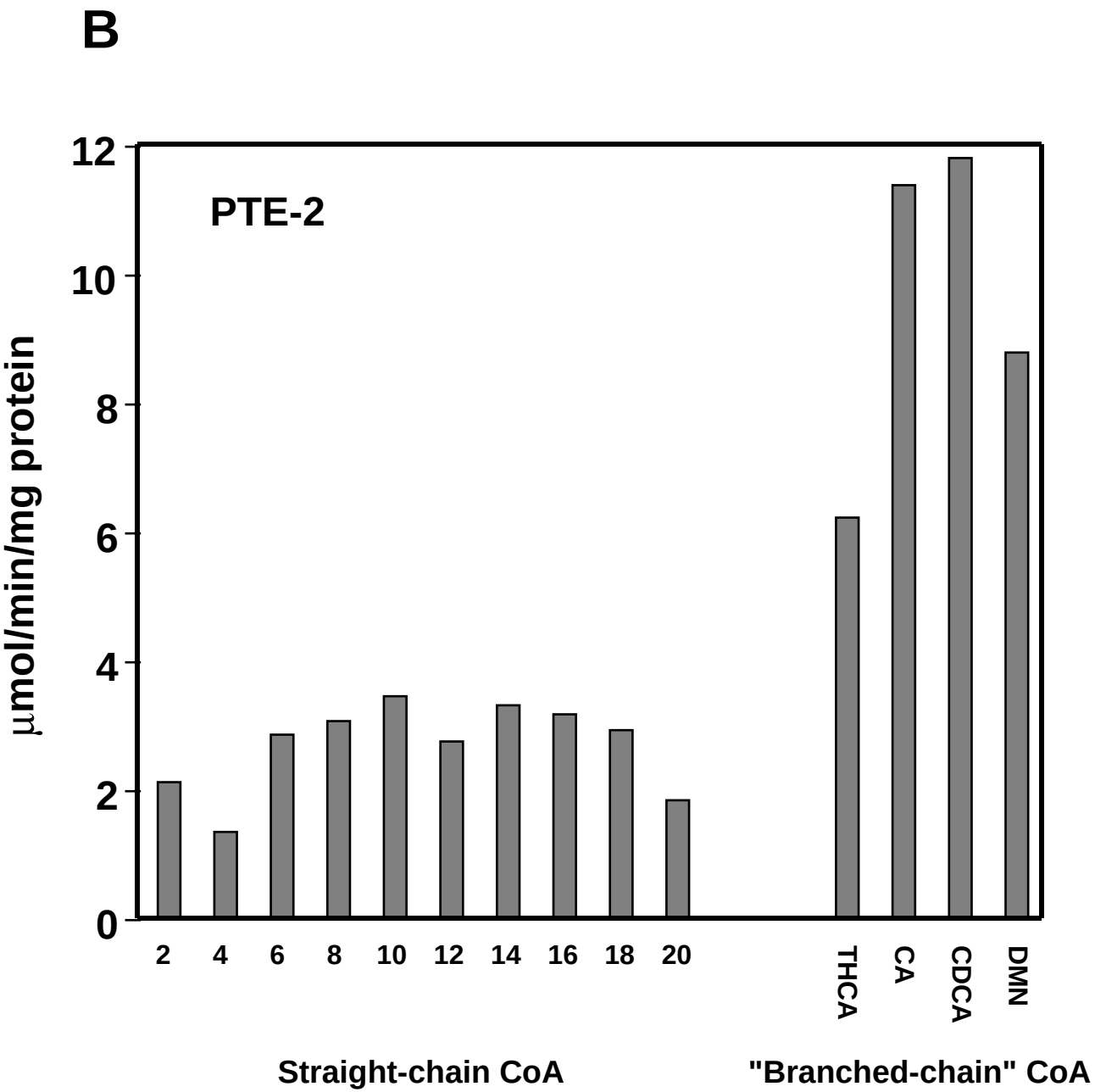

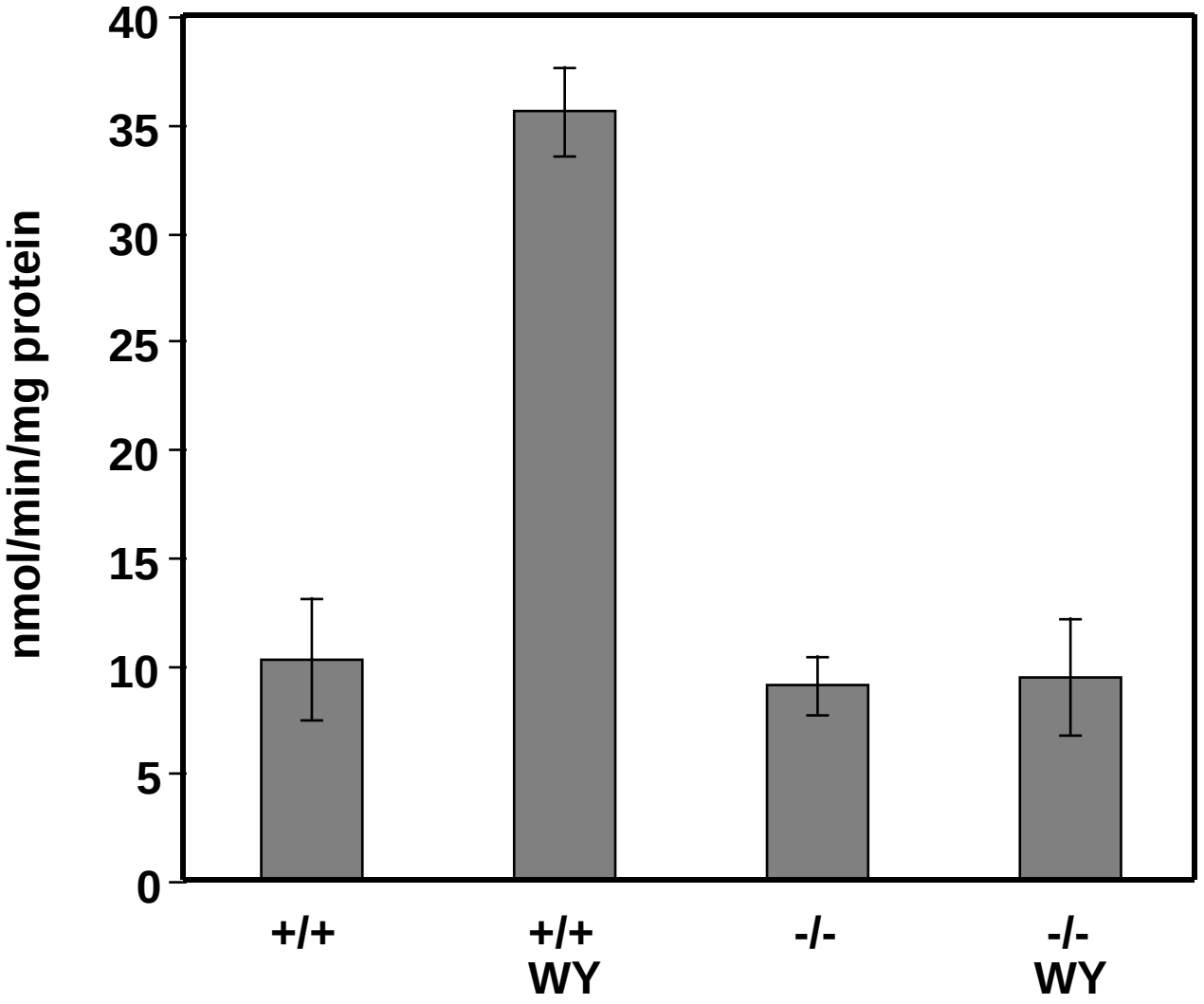
nmol/min/mg protein
40
35
30
25
20
15
10
5
0
+/+
+/+ WY
-/-
-/- WY

A

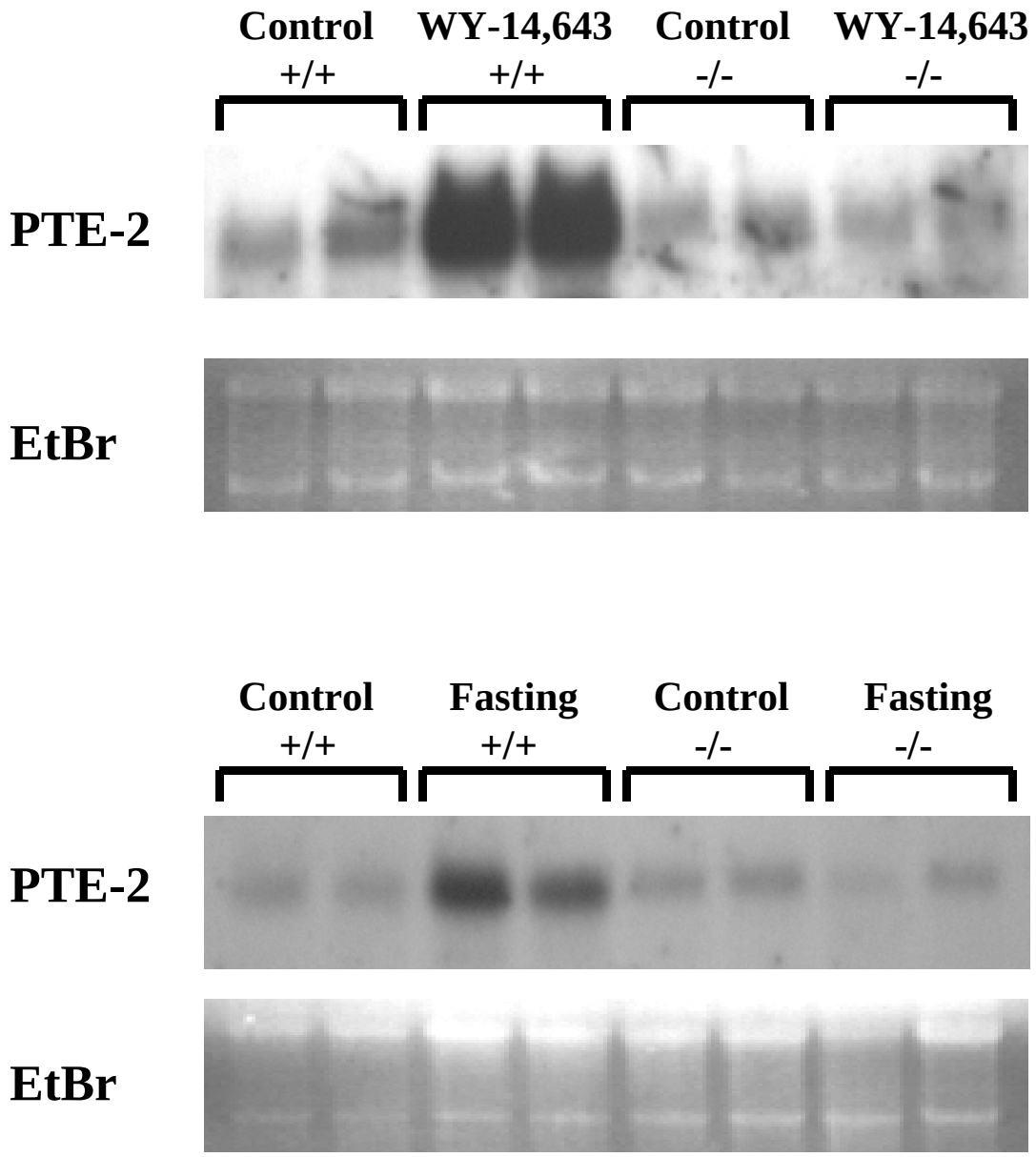
Control
WY-14,643
Control
WY-14,643
+/+
+/+
-/-
-/-
PTE-2
EtBr
Control
Fasting
Control
Fasting
+/+
+/+
-/-
-/-
PTE-2
EtBr

Hunt et al
Fig. 7B

B

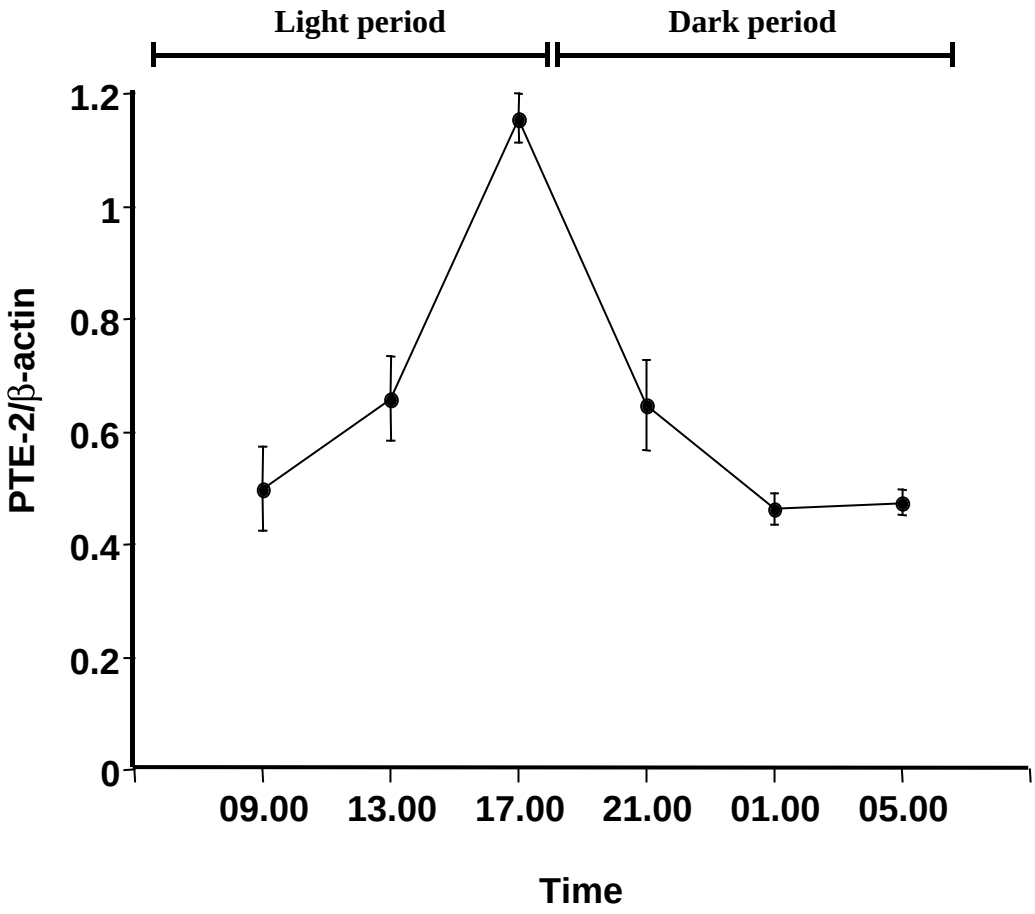

Hunt et al
Fig. 7C

C

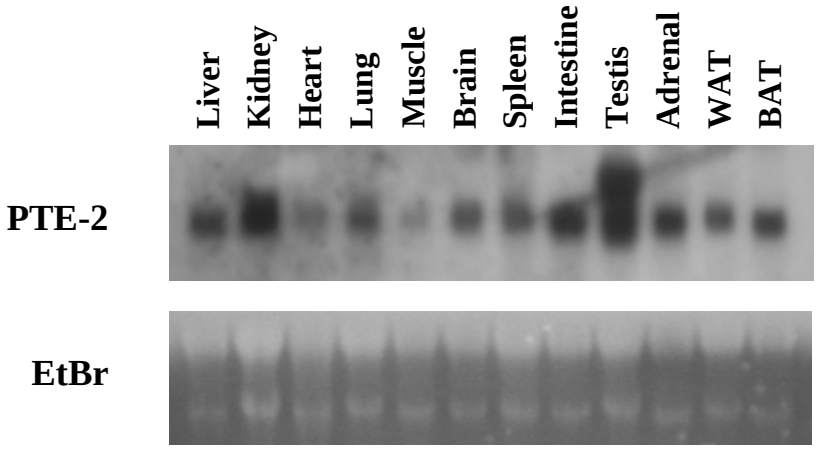

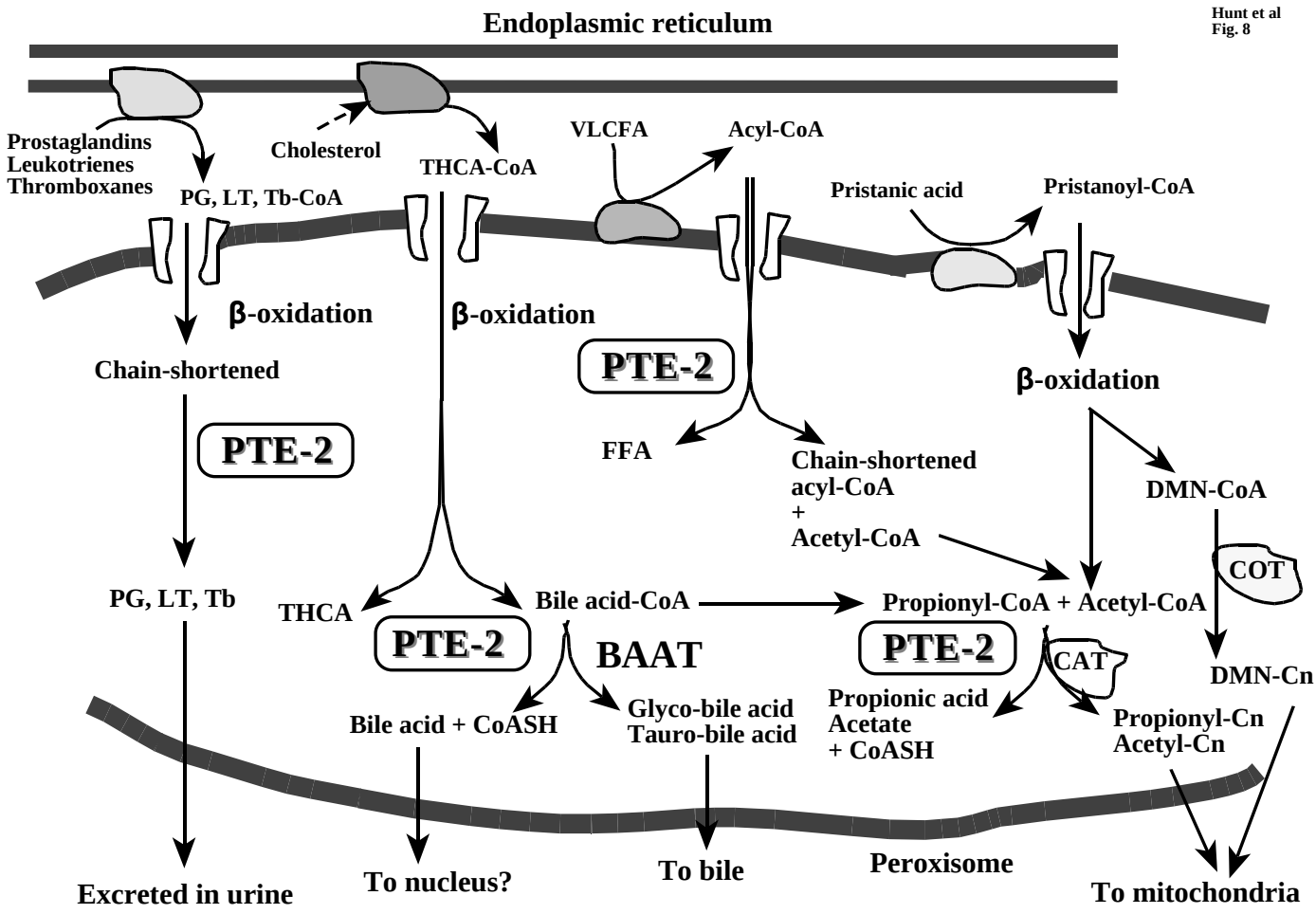
Endoplasmic reticulum
Hunt et al
Fig. 8
Prostaglandins
Leukotrienes
Thromboxanes
Cholesterol
THCA-CoA
VLCFA
Acyl-CoA
PG, LT, Tb-CoA
Pristanic acid
Pristanoyl-CoA
β-oxidation
β-oxidation
Chain-shortened
PTE-2
PTE-2
FFA
Chain-shortened
acyl-CoA
+
Acetyl-CoA
β-oxidation
DMN-CoA
COT
PG, LT, Tb
THCA
PTE-2
Bile acid-CoA
BAAT
Propionyl-CoA + Acetyl-CoA
PTE-2
CAT
DMN-Cn
Bile acid + CoASH
Glyco-bile acid
Tauro-bile acid
Propionic acid
Acetate
+ CoASH
Propionyl-Cn
Acetyl-Cn
Excreted in urine
To nucleus?
To bile
Peroxisome
To mitochondria